

# Why Can't I Open My Drawer? Mitigating Object-Driven Shortcuts in Zero-Shot Compositional Action Recognition

Geo Ahn<sup>1\*</sup>, Inwoong Lee<sup>2</sup>, Taeh Kim<sup>2</sup>, Minho Shim<sup>2</sup>, Dongyoon Wee<sup>2</sup>, and  
Jinwoo Choi<sup>1†</sup>

<sup>1</sup>Kyung Hee University    <sup>2</sup>NAVER Cloud  
{ahngeo11, jinwoochoi}@khu.ac.kr

**Abstract.** Zero-Shot Compositional Action Recognition (ZS-CAR) requires recognizing novel verb–object combinations composed of previously observed primitives. In this work, we tackle a key failure mode: models predict verbs via *object-driven shortcuts* (*i.e.*, relying on the labeled object class) rather than temporal evidence. We argue that sparse compositional supervision and verb–object learning asymmetry can promote object-driven shortcut learning. Our analysis with proposed diagnostic metrics shows that existing methods overfit to training co-occurrence patterns and underuse temporal verb cues, resulting in weak generalization to unseen compositions. To address object-driven shortcuts, we propose Robust COmpositional REpresentations (**RCORE**) with two components. Co-occurrence Prior Regularization (CPR) adds explicit supervision for unseen compositions and regularizes the model against frequent co-occurrence priors by treating them as hard negatives. Temporal Order Regularization for Composition (TORC) enforces temporal-order sensitivity to learn temporally grounded verb representations. Across Sth-com and EK100-com, **RCORE** reduces shortcut diagnostics and consequently improves compositional generalization.

**Keywords:** Zero-shot compositional action recognition · Compositional generalization · Video representation learning

## 1 Introduction

Many human actions can be decomposed into two semantic primitives—verbs and objects—and robust video understanding requires recognizing each component and reasoning over their interaction as a composition [3, 8, 9, 13, 28]. Zero-Shot Compositional Action Recognition (ZS-CAR) formalizes this goal: a model must recognize unseen verb–object pairs while keeping the verb and object vocabularies shared across splits [16, 17, 20, 44].

---

\*This work was done during an internship at NAVER Cloud.

†Corresponding author.

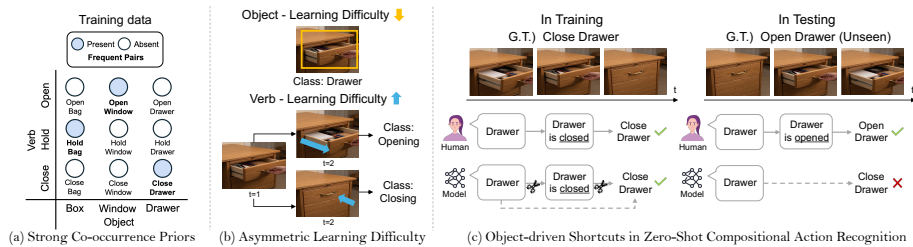


**Fig. 1: Why object-driven shortcuts emerge in compositional video understanding?** (a) **Co-occurrence bias.** Datasets are intrinsically sparse and highly skewed in their verb-object combinations, creating strong co-occurrence priors. (b) **Asymmetric learning difficulty.** Objects are visually explicit and easy to recognize from a single frame, whereas verbs require multi-frame temporal reasoning. This imbalance makes object features dominate training signals. (c) **Object-driven shortcuts.** Together, these two factors drive models to adopt *object-driven shortcuts*, hindering genuine compositional generalization. Once the object is recognized, the model often predicts the most frequent verb paired with it, ignoring temporal evidence.

In this setting, a key failure mode emerges: models often predict verbs via *object-driven shortcuts* rather than temporal evidence. Throughout, *object* refers to the *labeled noun class* in the verb-object vocabulary (not unlabeled background entities). We argue that object-driven shortcuts arise from two issues inherent to ZS-CAR.

First, **compositional supervision is sparse and skewed**. As illustrated in Figure 1 (a), datasets cover only a small fraction of the combinatorial verb-object space, and training labels concentrate on a limited set of frequent pairs [8, 28]. This skew induces a strong *co-occurrence prior* in the *training data*—the empirical dominance of frequent verb-object pairs—which can be amplified into a *model shortcut* at training time. Under such skewed supervision, predictions for unseen compositions tend to drift toward *seen* (especially frequent) pairs. Second, **verbs are harder to learn than objects**. As shown in Figure 1 (b), an object often becomes recognizable from a single frame, whereas a verb typically requires multi-frame temporal reasoning. Prior work on shortcut learning suggests that models tend to rely on easier-to-learn cues rather than the intended evidence [12, 21, 31, 36, 38]. In ZS-CAR, this verb-object difficulty gap makes object cues an especially attractive shortcut for verb prediction.

In this work, we posit that these two intertwined issues in verb-object compositional learning promote *object-driven shortcuts*, which we diagnose as the key factor hindering ZS-CAR. As Figure 1 (c) illustrates, a model can match a verb once it recognizes its frequently co-occurring object during training, without modeling the temporal dynamics essential to correctly recognize the verb. This behavior weakens generalization to unseen compositions because it ties verb prediction to object-dependent priors rather than temporally grounded evidence. We observe that models [20], even with a modern video-pretrained backbone [41], indeed confuse verbs with opposite temporal order (*e.g.*, opening *vs.* closing) on unseen compositions (see Section 5.2).

To dissect how object-driven shortcuts hinder unseen generalization, we perform a comprehensive quantitative diagnosis. First, through controlled experiments, we show that the asymmetric learning difficulty between verbs and objects, together with skewed co-occurrence priors, promotes verb shortcut learning driven by object cues. Next, we *quantify* shortcut-driven failures in existing ZS-CAR models by two diagnostic ratios: False Seen Prediction (FSP) and False Co-occurrence Prediction (FCP), which measure how often an unseen input collapses to a seen—and especially frequent—training composition. Using FSP/FCP, we show that a strong ZS-CAR baseline [20] remains heavily biased toward seen compositions, resulting in poor generalization to unseen compositions.

Driven by the diagnosis, we propose Robust COmpositional REpresentations (RCORE), targeting the two root causes of object-driven shortcuts. First, Co-occurrence Prior Regularization (CPR) expands supervision over originally absent compositions and suppresses the dominance of frequently seen pairs by treating them as hard negatives. Second, Temporal Order Regularization for Composition (TORC) enforces temporal-order sensitivity so that the model learns temporally grounded verb representations instead of relying on static cues.

We validate RCORE on Sth-com [20] under a realistic open-world evaluation protocol that evaluates all possible verb-object pairs, without requiring test-set ground truth labels. We also introduce EK100-com, a ZS-CAR dataset repurposed from EPIC-KITCHENS-100 [8], which exhibits more severe compositional sparsity than Sth-com [20]. Across datasets and backbones, RCORE reduces shortcut diagnostics (FSP/FCP) and improves unseen compositional generalization.

In this work, we make the following major contributions:

- **Shortcut Diagnosis:** We provide a diagnostic view of *object-driven shortcuts* in ZS-CAR. We empirically identify strong co-occurrence priors and asymmetric learning difficulty as the root causes of the shortcuts. Furthermore, we expose the limitations of baselines by quantifying how unseen inputs collapse into seen—especially frequent-training pairs, using FSP/FCP.
- **Diagnosis-Driven Framework:** We propose RCORE comprising CPR to suppress co-occurrence priors by expanding supervision over originally absent compositions and TORC to promote temporally grounded verb learning.
- **Effectiveness & Robustness:** We demonstrate that RCORE is effective, achieving superior performance on unseen compositions over baselines on Sth-com and EK100-com datasets, with multiple VLM backbones. Moreover, through extensive quantitative analyses, we prove that our approach mitigates co-occurrence biases and learns temporally grounded verb features.

## 2 Related Work

**Compositional Action Recognition (CAR).** CAR aims to recognize actions by factoring them into verbs and objects. A recurring challenge is learning verb representations that are robust to static cues (*e.g.* objects/scenes) and capture temporal dynamics [6, 28, 39]. Prior work addresses this by modeling object-level interactions [28, 39] or by training verb representations to be less sensitive to

object appearance [6]. Related directions include *open-vocabulary* CAR, which expands the action label space beyond a fixed taxonomy (often via text-driven semantics) [6,25]. In this work, we study Zero-Shot Compositional Action Recognition (ZS-CAR) under a fixed verb/object vocabulary, where verb and object label sets are shared across splits but some verb-object *pairs are held out* for testing [16,17,20,44]. In ZS-CAR, conditional learning [16,20] and disentanglement-oriented designs [17] improve joint modeling, yet our study highlights that these models can still exhibit *object-driven shortcut* behavior under sparse and skewed compositional supervision (see Section 3, Section 5.2).

**Compositional Zero-Shot Learning (CZSL) for image understanding.**

In the image domain, CZSL focuses on recognizing novel compositions of seen primitives (*e.g.*, attribute-object) under sparse compositional supervision [18,27,29,30,32,42]. Representative approaches include feature disentanglement [35,48], modular factorization [33], and CLIP-based prompt learning [22,32]. Compared to image CZSL, ZS-CAR additionally requires temporal grounding of verbs, which changes both the failure modes and the regularization opportunities. In contrast, we reveal how sparse compositional supervision, coupled with the higher learning difficulty of verbs, amplifies shortcut reliance in videos, and propose training-time regularizers tailored to ZS-CAR.

**Shortcut learning.** Models can learn *shortcuts* by exploiting spurious correlations that are easier to fit than the intended evidence [12,15,31,36]. Such shortcuts are closely tied to skewed training distributions and co-occurrence statistics, which can induce reliance on dataset priors [2,38]. In compositional settings, prior work reweights rare combinations to mitigate co-occurrence bias [18]. In video understanding, several works report reliance on static cues such as scenes [3,7,10,40] and objects [4,6] instead of motion-sensitive evidence. Building on these observations, we study a ZS-CAR-specific manifestation: *object-driven shortcuts* where object cues dominate verb prediction under sparse verb-object supervision, and we quantify this behavior with dedicated diagnostics.

**Vision-Language Model (VLM).** Recent VLMs broadly follow two paradigms: encoder-based and decoder-based. CLIP [34] is a representative encoder-only VLM pretrained via large-scale contrastive learning, and it exhibits strong zero-shot recognition [34] as well as non-trivial compositional behavior [1]. Following CLIP, recent works pretrain encoder-based video VLMs on large-scale video-text data [19,26,41,49]. Decoder-based VLMs (*e.g.*, LLaVA [23], Qwen-VL [5]) couple a vision encoder with an LLM decoder and excel at open-ended generation. In ZS-CAR, however, inference and evaluation operate over a *fixed* verb-object label space with *explicit compositional scores* (*i.e.*, logits over  $\mathbb{Y}^V \times \mathbb{Y}^O$ ), which provides a controlled interface for diagnosis and for designing training-time regularizers that are *transferable across backbones*. Such decoder-based VLM interfaces often do not expose, in a standardized and reproducible way, explicit scores over the fixed label space, as they primarily provide language outputs at inference time. Therefore, we focus on encoder-based VLMs in this controlled setting, and show that object-driven shortcuts persist even with a video-pretrained

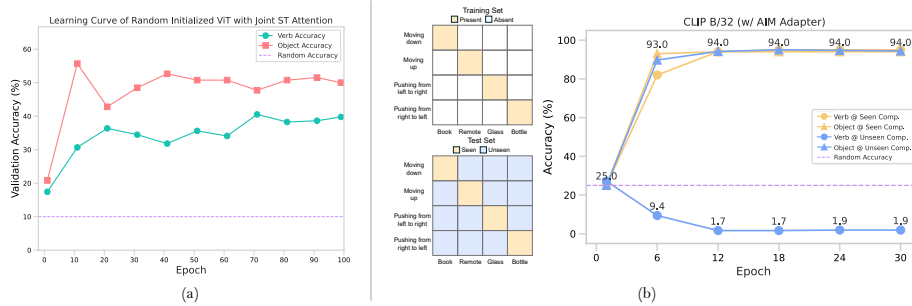


**Fig. 2: Controlled experiments demonstrate object-driven shortcut.** (a) **Objects are easier than verbs.** A randomly initialized ViT trained on a balanced  $10 \times 10$  Sth-com subset learns objects substantially faster than verbs. (b) **Co-occurrence bias induces object-driven shortcuts.** On a perfectly biased training split, CLIP (with AIM [43]) achieves high object accuracy, but verb accuracy on bias-conflict unseen compositions drops below chance, indicating shortcut-driven verb failures.

backbone [41] when paired with a strong ZS-CAR baseline [20]; we then propose RCORE to regularize compositional scoring to mitigate these shortcuts.

### 3 Diagnosis: Why ZS-CAR Models Fail?

#### 3.1 Zero-Shot Compositional Action Recognition

We study Zero-Shot Compositional Action Recognition (ZS-CAR) [20], where the goal is to recognize *unseen verb-object compositions* that are held out from the training set, while the verb and object vocabularies are *fixed* and shared across train/validation/test splits. Thus, unlike open-set or open-vocabulary settings, ZS-CAR does not introduce unseen *verbs* or *objects* at test time—only unseen *compositions* (verb-object pairs). Let  $\mathbb{Y}^V$  and  $\mathbb{Y}^O$  denote the sets of verb and object labels, and let each composition label be a pair  $\mathbf{y}^C = (\mathbf{y}^V, \mathbf{y}^O) \in \mathbb{Y}^V \times \mathbb{Y}^O$ . The training set is  $\mathbb{D}_{\text{train}} = \{(\mathbf{X}_i, \mathbf{y}_i^C)\}_{i=1}^N$ , and its set of observed (seen) compositions is  $\mathbb{Y}_{\text{seen}} = \{\mathbf{y}_i^C \mid (\mathbf{X}_i, \mathbf{y}_i^C) \in \mathbb{D}_{\text{train}}\}$ . The space of unseen compositions is  $\mathbb{Y}_{\text{unseen}} = (\mathbb{Y}^V \times \mathbb{Y}^O) \setminus \mathbb{Y}_{\text{seen}}$ . The validation and test sets contain both seen and unseen compositions, enabling evaluation of compositional generalization.

#### 3.2 Diagnostic Metrics

To better understand ZS-CAR model behavior, we introduce two diagnostics: (1) *training-bias* metrics that quantify over-reliance on training co-occurrence statistics, and (2) the *Compositional Gap* that measures the benefit of modeling verb-object dependence beyond independent recognition.

**Training-bias metrics.** To quantify reliance on co-occurrence priors, we define two misclassification ratios on the *unseen* subset of an evaluation split  $\mathbb{Y}_{\text{unseen}}$ . *False Seen Prediction (FSP)* is the fraction of misclassified unseen composition samples whose predictions  $\hat{\mathbf{y}}^C$  fall into the seen composition categories  $\mathbb{Y}_{\text{seen}}$ . *False Co-occurrence Prediction (FCP)* is the fraction of misclassified unseen composition samples whose prediction  $\hat{\mathbf{y}}^C$  falls into the frequent compositions

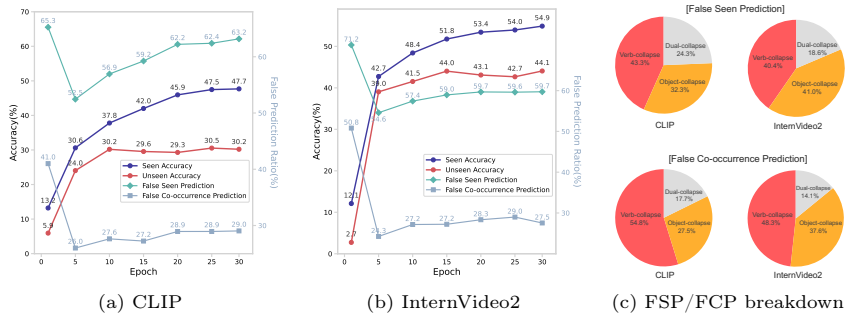


**Fig. 3: Shortcut reliance correlates with poor unseen generalization.** We show learning curves of C2C [20] on Sth-com with CLIP [34] and InternVideo2 [41]. (a) With CLIP, the seen–unseen accuracy gap grows together with FSP/FCP, indicating strong overfitting to seen compositions. (b) Even with the video-pretrained InternVideo2 backbone, the model still shows a notable seen–unseen gap and high FSP. (c) FSP/FCP breakdown at the final epoch: CLIP is dominated by verb-collapse due to object-driven shortcuts, while InternVideo2 exhibits milder but persistent shortcut behavior. Best viewed with zoom and color.

$\mathbb{Y}_{\text{freq}}$ . Let  $f(\mathbf{y}^C)$  denote the training frequency of a seen composition  $\mathbf{y}^C \in \mathbb{Y}_{\text{seen}}$ . We define the set of frequent seen compositions  $\mathbb{Y}_{\text{freq}}$  as

$$\mathbb{Y}_{\text{freq}} = \{\mathbf{y}^C \in \mathbb{Y}_{\text{seen}} \mid f(\mathbf{y}^C) > \mu_f + \sigma_f\}, \quad (1)$$

where  $\mu_f$  and  $\sigma_f$  are the mean and standard deviation of  $\{f(\mathbf{y}^C)\}_{\mathbf{y}^C \in \mathbb{Y}_{\text{seen}}}$ . To further analyze shortcut patterns, we decompose FSP/FCP into three component-wise cases based on prediction errors: (i) Verb-collapse, where the predicted object is correct but the verb is incorrect; (ii) Object-collapse, where the predicted verb is correct but the object is incorrect; and (iii) Dual-collapse, where both verb and object are incorrect. Using the metrics, we can identify whether co-occurrence bias primarily harms verb or object learning.

**Compositional Gap.** We introduce *Compositional Gap* ( $\Delta_{\text{CG}}$ ) to examine whether a model benefits from predicting the joint verb–object composition beyond getting the two components correct independently. Given joint logits over  $\mathbb{Y}^V \times \mathbb{Y}^O$ , we obtain the predicted composition  $\hat{\mathbf{y}}^C = (\hat{\mathbf{y}}^V, \hat{\mathbf{y}}^O)$  by selecting the top-1 composition label. We then compute top-1 accuracies  $\text{Acc}^V$ ,  $\text{Acc}^O$ , and  $\text{Acc}^C$  respectively. Then we define  $\Delta_{\text{CG}}$  as

$$\Delta_{\text{CG}} = \text{Acc}^C - (\text{Acc}^V \times \text{Acc}^O). \quad (2)$$

We report  $\Delta_{\text{CG}}$  alongside FSP/FCP and unseen composition accuracy as a *diagnostic* metric, rather than interpreting it as a standalone evaluation criterion.

### 3.3 Empirical Diagnosis of Object-driven Shortcuts in ZS-CAR

In this section, we empirically diagnose object-driven shortcut behavior in ZS-CAR and analyze how it correlates with weak verb learning and poor generalization to unseen compositions. We show that this behavior persists even with a

modern video-pretrained VLM backbone [41], and provide additional evidence in Section 5 and Section D.

**Objects are easier to learn than verbs.** To compare the learning difficulty of verbs and objects, we train a randomly initialized ViT [11] on a controlled subset of Sth-com [20]. Specifically, we construct a balanced  $10 \times 10$  subset containing all 100 verb-object pairs to isolate learning dynamics from compositional sparsity. Based on prior observations that models tend to fit easier cues earlier under limited supervision [31, 36], we compare the learning curves of verb *vs.* object prediction. In Figure 2 (a), the model learns objects faster and reaches higher accuracy than verbs under this controlled setting, suggesting that object prediction is easier than verb prediction in our ZS-CAR setup.

**Object-driven shortcuts indeed exist in ZS-CAR.** Under skewed co-occurrence statistics, models may rely on easier cues as shortcuts instead of learning the intended evidence [4, 7, 12, 21, 31, 36]. We test whether CLIP exhibits such object-driven shortcuts by constructing a *bias-controlled* training split where each verb is strongly correlated with a particular object (see construction details in Section C), and evaluating on two splits: (i) *bias-aligned* seen compositions and (ii) *bias-conflict* unseen compositions. As shown in Figure 2 (b), CLIP achieves high object accuracy *on unseen compositions* while verb accuracy *on unseen compositions* drops below the uniform-chance level ( $1/|\mathbb{Y}^V|$ ), indicating that object cues dominate verb prediction under this biased supervision. We observe this trend even with random initialization, implying shortcuts stem from the training distribution and objective, not just pretraining. See Section C for more details.

**Shortcut reliance correlates with poor unseen generalization.** Next, we test whether shortcut reliance correlates with weak unseen generalization in a standard SOTA pipeline. Figure 3 plots validation accuracies together with FSP/FCP for C2C [20] on Sth-com [20]. As shown in Figure 3 (a), with a CLIP backbone [34], increasing FSP/FCP accompanies a widening seen-unseen gap, consistent with growing reliance on co-occurrence statistics. Our error breakdown in Figure 3 (c) further shows that, among unseen samples that collapse to seen pairs, a large fraction corresponds to *verb-collapse*, supporting the presence of object-driven shortcut behavior. As shown in Figure 3 (b) and (c), with an InternVideo2 [41] backbone, the trends are more stable; however, FSP remains high, and the FCP breakdown still exhibits substantial verb-collapse, suggesting that stronger video pre-training alone is insufficient to eliminate the tendency to overfit to seen pairs via co-occurrence-driven shortcuts.

**$\Delta_{CG}$  indicates degraded compositional behavior on unseen compositions.** We report  $\Delta_{CG}$  of C2C [20] with CLIP [34] and InternVideo2 [41] backbones. As shown in Table 1, the model exhibits negative  $\Delta_{CG}$  on unseen compositions even with the video-pretrained backbone, indicating that  $\text{Acc}^C$  falls below the independent reference  $\text{Acc}^V \times \text{Acc}^O$ . Together with the training-bias metrics (FSP/FCP), these results support that

**Table 1:  $\Delta_{CG}$  on Sth-com.**

Backbone	Split	$\Delta_{CG}$
CLIP	Seen	+3.24
	Unseen	-0.42
InternVideo2	Seen	+2.24
	Unseen	-0.63

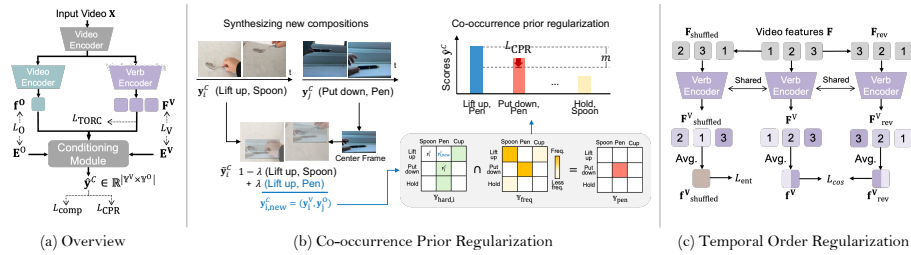


**Fig. 4: Overview of RCORE.** (a) Overview of our proposed RCORE framework. (b) CPR synthesizes plausible yet unseen verb–object compositions and penalizes frequently seen hard negatives by a margin-based regularizer. (c) TORC penalizes alignment between original and temporally perturbed feature vectors, enforcing explicit temporal order modeling and reducing object-driven shortcuts.

shortcut reliance is closely associated with weak unseen compositional generalization in current ZS-CAR pipelines.

## 4 RCORE

We introduce RCORE, a diagnosis-driven learning framework that mitigates *object-driven shortcuts* in ZS-CAR. RCORE improves compositional generalization by strengthening verb–object representations under sparse supervision through two complementary components: (i) Co-occurrence Prior Regularization (CPR) expands supervision over novel compositions and leverages frequently seen pairs as hard negatives to suppress co-occurrence priors, and (ii) Temporal Order Regularization for Composition (TORC) loss promotes temporally grounded verb learning over static object cues. Following prior work [17, 20], we employ an adapter-based tuning, AIM [43] for CLIP [34] and LoRA [14] for InternVideo2 [41], as our backbone. Figure 4 (a) gives an overview of RCORE.

**Feature extraction.** Given a video  $\mathbf{X}$  with  $T$  frames, the backbone encoder outputs frame-level features  $\mathbf{F} \in \mathbb{R}^{T \times D}$ . We transform them into verb features  $\mathbf{F}^V \in \mathbb{R}^{T \times D}$  and object features  $\mathbf{f}^O \in \mathbb{R}^D$  using dedicated encoders. We obtain text embeddings for verbs and objects,  $\mathbf{E}^V \in \mathbb{R}^{|\mathbb{Y}^V| \times D}$  and  $\mathbf{E}^O \in \mathbb{R}^{|\mathbb{Y}^O| \times D}$ , by feeding class-specific prompts into the text encoder.

### 4.1 CPR: Co-occurrence Prior Regularization

To mitigate object-driven shortcuts under sparse and skewed compositional supervision, we propose CPR, a training strategy that injects supervision for *synthesized* verb–object pairs while preserving the stability of closed-world optimization. CPR combines (i) synthesized composition supervision, (ii) a margin-based regularizer that down-weights *frequently* seen hard negatives, and (iii) a batch-adaptive expansion of the composition label space to make these new pairs trainable without optimizing over the full  $\mathbb{Y}^V \times \mathbb{Y}^O$  space.

**Synthesized composition supervision.** To provide explicit supervision for compositions absent from the training set, we first synthesize videos that represent new *composition* labels. Given a training sample  $\mathbf{X}_i$  with composition label  $\mathbf{y}_i^C = (\mathbf{y}_i^V, \mathbf{y}_i^O)$ , we construct a new video  $\tilde{\mathbf{X}}_i$  by injecting the static object cue

from another video  $\mathbf{X}_j$  (with  $\mathbf{y}_j^O \neq \mathbf{y}_i^O$ ) into the high-motion regions of  $\mathbf{X}_i$ , as shown in Figure 4 (b). Specifically, for each frame  $k \in \{1, \dots, T\}$  we obtain

$$\tilde{\mathbf{X}}_i^k = (\mathbf{1} - \lambda \mathbf{M}_i^k) \odot \mathbf{X}_i^k + (\lambda \mathbf{M}_i^k) \odot \mathbf{X}_j^{\lfloor T/2 \rfloor}, \quad (3)$$

where  $\lambda \in [0, 1]$  controls the injection strength and  $\mathbf{M}_i^{(k)} \in \{0, 1\}^{H \times W}$  is the high-motion region mask for frame  $k$ , extracted by a learning-free estimator [10]. The operator  $\odot$  denotes element-wise multiplication, with  $\mathbf{M}_i^k$  broadcast across channels. Accordingly, we use soft labels for the synthesized video as follows:

$$\tilde{\mathbf{y}}_i^O = (1 - \lambda) \mathbf{y}_i^O + \lambda \mathbf{y}_j^O, \quad (4)$$

$$\tilde{\mathbf{y}}_i^C = (1 - \lambda) \phi(\mathbf{y}_i^V, \mathbf{y}_i^O) + \lambda \phi(\mathbf{y}_i^V, \mathbf{y}_j^O), \quad (5)$$

where  $\phi : \mathbb{Y}^V \times \mathbb{Y}^O \rightarrow \{0, 1\}^{|\mathbb{Y}^V \times \mathbb{Y}^O|}$  maps a composition  $(\mathbf{y}^V, \mathbf{y}^O)$  to its one-hot vector in the flattened joint label space.

**Co-occurrence prior regularization loss.** Even after adding supervision for synthesized compositions, skewed co-occurrence statistics can still make the model over-score a small set of *frequently* seen pairs. To counter this score collapse, we enforce a margin constraint that makes the *target synthesized* composition  $\mathbf{y}_{i,\text{new}}^C = (\mathbf{y}_i^V, \mathbf{y}_j^O)$  outrank *frequent seen hard negatives* by at least  $m$ . We define the hard-negative label set for  $\mathbf{y}_{i,\text{new}}^C$  as follows:

$\mathbb{Y}_{\text{hard},i} = \{(\mathbf{y}^V, \mathbf{y}^O) \mid [(\mathbf{y}^V = \mathbf{y}_i^V) \oplus (\mathbf{y}^O = \mathbf{y}_j^O)] \setminus (\mathbf{y}^V, \mathbf{y}^O) \neq (\mathbf{y}_i^V, \mathbf{y}_i^O)\}$ , (6) where  $\oplus$  denotes the exclusive or operator. Let  $\mathbb{Y}_{\text{freq}} \subset \mathbb{Y}_{\text{seen}}$  be the set of frequently seen compositions (details about the criterion in Section C.2). Then we define the CPR loss with margin  $m$  over the penalty set  $\mathbb{Y}_{\text{pen}} = \mathbb{Y}_{\text{hard},i} \cap \mathbb{Y}_{\text{freq}}$  as:

$$L_{\text{CPR}} = \sum_{\mathbf{y}^C \in \mathbb{Y}_{\text{pen}}} \max\left(0, s(\mathbf{y}^C) - s(\mathbf{y}_{i,\text{new}}^C) + m\right), \quad (7)$$

where  $s(\mathbf{y}^C)$  denotes the logit assigned to the composition label  $\mathbf{y}^C$ .

**Batch-adaptive label-space expansion.** Conventional ZS-CAR pipelines optimize classification only over *seen* compositions  $\mathbb{Y}_{\text{seen}}$  (closed-world over compositions), which makes it non-trivial to directly supervise *novel* verb-object pairs during training. On the other hand, naively applying cross-entropy over the full  $\mathbb{Y}^V \times \mathbb{Y}^O$  space can harm unseen accuracy by treating most unseen compositions as negatives throughout training (see Section 5.4). To provide an effective supervision for novel compositions, we introduce a *batch-adaptive label space expansion* strategy. For each mini-batch, we construct an expanded label set as  $\mathbb{Y}_{\text{exp}} = \mathbb{Y}_{\text{seen}} \cup \mathbb{Y}_{\text{new}}$ , where  $\mathbb{Y}_{\text{new}}$  denotes the label set for the newly synthesized videos. We compute cross-entropy only over  $\mathbb{Y}_{\text{exp}}$ . This preserves the optimization stability of closed-world training while progressively injecting supervision for new compositions.

## 4.2 TORC: Temporal Order Regularization for Composition

To counter object-driven shortcuts in verb learning, we introduce TORC, a temporal *order-sensitivity* regularizer. While CPR expands supervision over compositions, verb recognition can still collapse to static object cues due to the asymmetric learning difficulty between verbs and objects. As shown in Figure 4 (c), TORC directly regularizes the verb representation to depend on temporal structure: it (i) discourages invariance to temporal reversal by separating forward and reversed features, and (ii) penalizes over-confident verb predictions when temporal order is disrupted by encouraging high-entropy outputs. Together, these constraints reduce reliance on static cues and promote temporally grounded verb representations.

**Temporal perturbation for regularization.** Given frame-level features  $\mathbf{F} = (\mathbf{f}_1, \dots, \mathbf{f}_T)$ , we form two regularization views: (i) a reversed sequence  $\mathbf{F}_{\text{rev}} = (\mathbf{f}_T, \dots, \mathbf{f}_1)$ , and (ii) a temporally shuffled sequence  $\mathbf{F}_{\text{shuffled}} = \pi(\mathbf{F})$ , where  $\pi$  is a random permutation sampled from  $\mathcal{P}$ . We then feed  $\mathbf{F}_{\text{rev}}$  and  $\mathbf{F}_{\text{shuffled}}$  into the verb encoder to obtain perturbed verb features  $\mathbf{f}_{\text{rev}}^V \in \mathbb{R}^D$  and  $\mathbf{f}_{\text{shuffled}}^V \in \mathbb{R}^D$ .

**TORC loss.** We first push the model to distinguish forward and reversed temporal semantics. We minimize the cosine similarity between the original verb  $\mathbf{f}^V$  and the reversed feature vectors  $\mathbf{f}_{\text{rev}}^V$ :  $L_{\text{cos}} = \frac{\mathbf{f}^V \top \mathbf{f}_{\text{rev}}^V}{\|\mathbf{f}^V\| \|\mathbf{f}_{\text{rev}}^V\|}$ . Temporal reversal often flips action meaning (*e.g.*, opening *vs.* closing), yet the state-of-the-art model [20] yields a high cosine similarity (0.91; see Figure 13), indicating weak temporal discrimination.

Next, we regularize the model to avoid confident verb predictions when temporal structure is disrupted. Given the verb text embeddings  $\mathbf{E}^V = \{\mathbf{e}_m^V\}_{m=1}^{|\mathbb{Y}^V|}$ , we define the negative entropy loss  $L_{\text{ent}} = \sum_{m=1}^{|\mathbb{Y}^V|} p_m \log p_m$  with the predicted probability  $p_m$  of the  $m$ -th verb class based on the cosine similarity between visual and textual features as:

$$p_m = \frac{\exp(\cos(\mathbf{f}_{\text{shuffled}}^V, \mathbf{e}_m^V)/\tau)}{\sum_{n=1}^{|\mathbb{Y}^V|} \exp(\cos(\mathbf{f}_{\text{shuffled}}^V, \mathbf{e}_n^V)/\tau)}, \quad (8)$$

where  $\tau$  is a temperature parameter. Maximizing entropy prevents the model from inferring verbs from static spatial cues alone, enforcing reliance on temporal evidence. We define the TORC loss as:  $L_{\text{TORC}} = L_{\text{cos}} + L_{\text{ent}}$ .

## 4.3 Training

**Component loss.** We compute verb logits  $\mathbf{S}_V \in \mathbb{R}^{|\mathbb{Y}^V|}$  and object logits  $\mathbf{S}_O \in \mathbb{R}^{|\mathbb{Y}^O|}$  based on the cosine similarity scores. We apply standard cross-entropy losses for verb and object prediction:  $L_{\text{com}} = L_V + L_O$ .

**Composition loss.** Following prior work [20], we obtain the composition logits  $\mathbf{S}_C \in \mathbb{R}^{|\mathbb{Y}^V \times \mathbb{Y}^O|}$  by aggregating factorized logits:  $\mathbf{S}_C = \mathbf{S}_V \boxplus \mathbf{S}_{O|V} + \mathbf{S}_O \boxplus \mathbf{S}_{V|O}$ , where  $\mathbf{S}_{O|V}$  and  $\mathbf{S}_{V|O}$  represent the conditional logits and  $\boxplus$  denotes broadcasted addition into the joint verb-object space. Then we employ the cross-entropy loss integrated with our batch-adaptive label space expansion (Section 4.1). Given

$\mathbf{s}_c \in \mathbf{S}_C$ , the final composition loss utilizing the dynamically constructed denominator  $\mathbb{Y}_{\text{exp}}$  is formulated as:  $L_{\text{comp}} = -\log(\exp(\hat{s}_c) / \sum_{c=1}^{|\mathbb{Y}_{\text{exp}}|} \exp(s_c))$ .

**Total loss.** We train RCORE with the combined objective  $L_{\text{total}}$  defined as  $L_{\text{total}} = \alpha L_{\text{com}} + \beta L_{\text{comp}} + \gamma L_{\text{TORC}} + \delta L_{\text{CPR}}$ , where  $\alpha$ ,  $\beta$ ,  $\gamma$  and  $\delta$  are hyperparameters.

## 5 Experimental Results

Building on our diagnosis, we evaluate whether RCORE reduces shortcut reliance and improves compositional generalization. We first describe the experimental setup (Section 5.1), then present diagnostic analyses (Section 5.2), followed by quantitative comparisons (Section 5.3), and finally ablation studies (Section 5.4).

### 5.1 Experimental setup

**Limitations of conventional evaluation.** Existing ZS-CAR works [16, 17, 20] rely on the *closed-world* protocol, where inference is restricted to compositions that appear in the validation/test split. This protocol hides a model’s tendency to over-predict seen compositions and obscures co-occurrence-driven behaviors. More critically, *test-set-tuned* bias calibration selects a bias term using test labels, inflating unseen accuracy and undermining fair comparison.

**Our evaluation setup.** To expose genuine generalization, we adopt an *open-world, unbiased* protocol by default: (i) inference spans the full space  $\mathbb{Y}^V \times \mathbb{Y}^O$ , and (ii) no test labels are used to tune biases. We also report closed-world H.M. and AUC for comparison with existing methods. We show open-world biased results using a realistic validation set-tuned bias in Section E.4.

**Datasets.** We evaluate on two ZS-CAR benchmarks: Sth-com [20] and our curated EK100-com. Sth-com is derived from Something-Something V2 [13] and Something-Else [28], containing 79K videos with 161 verbs and 248 objects. Following prior work [37, 46], we also evaluate on the *Temporal* subset consisting of verbs requiring temporal reasoning. We additionally introduce the **EPIC-KITCHENS-100-composition (EK100-com)** dataset, constructed by repurposing EK100 [8] following the Sth-com protocol. EK100-com includes 71K egocentric videos, 82 verbs, and 228 objects. Due to the long-tailed label distribution of EK100, it exhibits *severe compositional sparsity*. Its label coverage ratio is only 7.5%, which is considerably lower than the 12.8% observed in Sth-com [20]. Full details are in Section B.

**Evaluation metrics.** We report top-1 composition, verb and object accuracies. Verb and object accuracies are conditioned on the *seen/unseen composition*: *verb@seen-comp* and *object@seen-comp* are computed on samples with  $\mathbf{y}^C \in \mathbb{Y}_{\text{seen}}$ , while *verb@unseen-comp* and *object@unseen-comp* are computed on samples with  $\mathbf{y}^C \in \mathbb{Y}_{\text{unseen}}$ . We report the corresponding harmonic mean (H.M.) between seen-comp and unseen-comp accuracies for composition, verb, and object. We also report the compositional gap  $\Delta_{\text{CG}}$  (2). For a detailed illustration of our evaluation setting, please refer Section A.

**Baselines.** We employ two encoder-based VLMs, CLIP-B/16 [34] and InternVideo2-CLIP-B/14 [41], as backbones for ZS-CAR methods. We put the InternVideo2-1B [41] backbone results in the supplementary material. We primarily compare RCORE against C2C [20], the current SOTA ZS-CAR method. To isolate

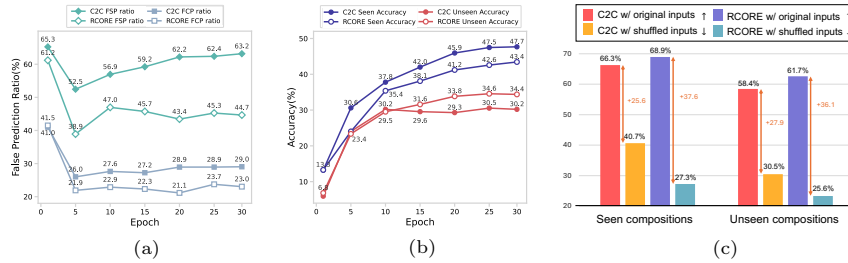


**Fig. 5: Analysis on the effects of RCORE on the Sth-com [20] dataset.** (a) RCORE suppresses the growth of FSP/FCP during training, unlike the baseline. (b) This reduces the seen–unseen gap and improves unseen composition accuracy. (c) On the temporal subset, RCORE shows a larger drop under temporal shuffling, indicating stronger temporal dependence over static cues. Best viewed with zoom and color.

the effect of conditional learning, we also evaluate the independent modeling baselines with CLIP [34] and InternVideo2 [41] backbones which are denoted as ‘AIM’ and ‘LoRA’, named after their respective adapter tuning methods, in Section 5.3. AIM [43] is the CLIP [34]-based spatio-temporal adapter model. We additionally include closed-world results of a recent ZS-CAR approach [17].

## 5.2 Analysis

We empirically show that RCORE reduces reliance on co-occurrence priors and mitigates object-driven shortcuts in verb learning, yielding more robust compositional behavior than the baseline [20]. Here, we present results with the CLIP [34] backbone, and we put InternVideo2 [41] results in the supplementary.

**RCORE less relies on co-occurrence prior.** In Figure 5 (a), we present the False Seen Prediction (FSP) and False Co-occurrence Prediction (FCP) curves of RCORE and the baseline [20] on Sth-com. While the baseline’s FSP and FCP increase substantially during training (53%  $\rightarrow$  63% and 26%  $\rightarrow$  29%), those of RCORE remain consistently lower and even decrease (47%  $\rightarrow$  44% and 23%  $\rightarrow$  23%), indicating markedly less dependence on co-occurrence statistics.

**Improved unseen generalization.**

In Figure 5 (b), we present the learning curve of our RCORE and the baseline [20] on Sth-com. RCORE significantly improves unseen composition accuracy upon the baseline (34% vs. 30%), and reduces the seen–unseen accuracy gap (9 points vs. 17 points).

**The learned verb representations are indeed effective.** Inspired by prior work [46], we evaluate models on the *Temporal* subset of Sth-com [20], as shown

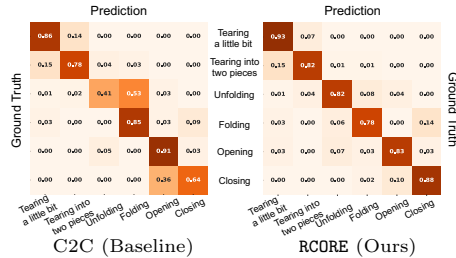


**Fig. 6: RCORE mitigates object-driven shortcuts in verb learning.** We visualize confusion matrices for six representative verbs on *unseen* compositions of the Sth-com [20] test set. All values are normalized frequencies across the six verb classes.

**Table 2: Sth-com [20] results.** We show the top-1 verb, object, and composition classification accuracy (%). We report performance on both seen and unseen compositions, along with their harmonic mean (H.M.).

Backbone	Method	Verb			Object			Composition		
		@Seen Comp	@Unseen Comp	H.M.	@Seen Comp	@Unseen Comp	H.M.	Seen ( $\Delta_{CG}$ )	Unseen ( $\Delta_{CG}$ )	H.M.
CLIP	AIM [43]	54.99	39.19	45.76	67.19	53.43	59.53	40.24 (+3.29)	18.50 (-2.44)	25.35
	C2C [20]	63.60	54.36	58.62	67.72	56.10	<b>61.36</b>	46.31 (+3.24)	30.08 (-0.42)	36.47
	RCORE	65.73	59.00	<b>62.18</b>	64.79	56.34	60.27	<b>44.99 (+2.40)</b>	<b>33.90 (+0.66)</b>	<b>38.67</b>
InternVideo2	LoRA [14]	48.83	36.50	41.78	64.79	58.61	61.55	32.83 (+1.19)	19.71 (-1.68)	24.63
	C2C [20]	70.35	63.29	66.63	70.03	63.44	<b>66.58</b>	51.50 (+2.24)	39.53 (-0.63)	44.73
	RCORE	71.65	66.65	<b>69.06</b>	67.96	64.56	66.22	<b>50.20 (+1.51)</b>	<b>43.98 (+0.95)</b>	<b>46.88</b>

in Figure 5 (c). Specifically, to measure a model’s dependence on static cues, we compare its performance when using temporally shuffled verb features  $\mathbf{f}_{\text{shuffled}}^V$  versus the original features  $\mathbf{f}^V$ . Across both seen and unseen compositions, RCORE exhibits a substantially larger performance gap between original and shuffled features. This demonstrates that its verb representations are effectively grounded in temporal dynamics.

In Figure 6, we visualize verb confusion matrices on *unseen* compositions of the Sth-com test set. RCORE discriminates pairs of opposite verbs, while C2C [20] frequently confuses them, *e.g.* misclassifying ‘unfolding’ as ‘folding’. These results collectively demonstrate that C2C fails to overcome the challenge of object-driven shortcuts in verb learning, whereas RCORE effectively mitigates it.

### 5.3 Comparisons with State-of-the-Art

**Sth-com.** As shown in Table 2, RCORE achieves clear gains on Sth-com [20] under a rigorous open-world setting. Compared to the C2C [20] baseline, RCORE improves the verb@unseen-comp by 4.6 points and the unseen composition accuracy by 3.8 points with the CLIP [34] backbone, and by 3.4 points and 4.5 points with InternVideo2 (IV2) [41], respectively. These gains are consistent with stronger verb recognition observed in our analysis (Section 5.2). Notably, RCORE yields a positive compositional gap ( $\Delta_{CG}$ ) on unseen compositions, whereas all baselines remain negative, indicating improved compositional behavior on unseen pairs. This improvement coincides with the highest composition H.M. under the open-world protocol. In Table 3, RCORE also records the highest H.M. and AUC under the closed-world, test-set-tuned protocol used in prior work [17].

**EK100-com.** Despite the strong co-occurrence prior in the EK100-com training compositions (see Section 5.1), RCORE achieves higher unseen composition accuracy and the best H.M. As shown in Table 4, compared to C2C [20], RCORE substantially improves unseen composition accuracy—by 6.9 points with the CLIP [34] backbone and 7.7 points with the IV2 [41] backbone—despite a decrease in seen composition accuracy. This pattern is consistent with reduced reliance on seen co-occurrence statistics and improved recognition of unseen com-

**Table 3: Closed-world results on Sth-com [20].**

Method	Closed-world	
	H.M.	AUC
AIM [43]	34.44	16.99
C2C [20]	42.75	23.77
Jung et al. [17]	42.60	23.50
RCORE	<b>43.21</b>	<b>25.27</b>

positions, along with their harmonic mean (H.M.).

**Table 4: EK100-com results.** We show the top-1 verb, object, and composition classification accuracy (%). We report performance on both seen and unseen compositions, along with their harmonic mean (H.M.).

Backbone	Method	Verb			Object			Composition		
		@Seen Comp	@Unseen Comp	H.M.	@Seen Comp	@Unseen Comp	H.M.	Seen ( $\Delta_{CG}$ )	Unseen ( $\Delta_{CG}$ )	H.M.
CLIP	AIM [43]	59.97	39.99	47.98	56.23	46.76	51.06	38.58 (+4.86)	14.98 (-3.71)	21.58
	C2C [20]	65.52	49.57	56.44	56.54	46.99	51.32	42.70 (+5.65)	21.56 (-1.73)	28.65
	RCORE	66.19	54.31	<b>59.66</b>	54.35	49.88	<b>52.02</b>	<b>39.70 (+3.73)</b>	<b>28.41 (+1.32)</b>	<b>33.12</b>
InternVideo2	LoRA [14]	59.73	32.99	42.51	51.08	39.34	44.45	36.43 (+5.92)	5.63 (-7.35)	9.75
	C2C [20]	68.95	57.01	62.41	60.54	52.31	56.12	47.30 (+5.55)	30.33 (+0.51)	36.96
	RCORE	69.00	60.98	<b>64.74</b>	56.59	56.40	<b>56.49</b>	<b>42.32 (+3.27)</b>	<b>38.07 (+3.68)</b>	<b>40.08</b>

positions. Moreover, RCORE yields a positive compositional gap ( $\Delta_{CG}$ ) on unseen compositions (+1.32 with CLIP and +3.68 with IV2), which is consistent with improved compositional behavior under highly sparse supervision.

#### 5.4 Ablation Studies

**Effects of RCORE components.** In Table 5 (a), using TORC alone yields the largest gain in verb generalization, improving *verb@unseen-comp* by 3.5 points, and gain in unseen composition accuracy by 3.8 points, compared to the baseline without CPR and TORC (C2C [20]). Using CPR alone primarily improves unseen composition accuracy by 3.1 points, while reducing seen composition accuracy 4.2 points, indicating a seen-unseen trade-off. Combining CPR and TORC achieves the best overall results, improving unseen composition accuracy by +5.0 points and composition H.M. by +2.7 points, suggesting complementary benefits of mitigating co-occurrence bias and enforcing temporal sensitivity.

**Effects of TORC components.** Table 5 (b) evaluates the roles of  $L_{cos}$ , which enforces discrimination of opposite temporal semantics, and  $L_{ent}$ , which prevents reliance on static cues. Each term individually improves performance, while using both terms yields the largest gains in the *verb@unseen-comp* (+3.5 points) and unseen composition accuracy (+3.8 points).

**Effects of label space in CPR.** In Table 5 (c), we validate the batch-adaptive label space expansion in CPR. Compared to closed-world training over  $\mathbb{Y}_{seen}$ , our batch-adaptive label space improves unseen composition accuracy (+2.3 points) and H.M. by injecting supervision for synthesized compositions while avoiding unstable optimization. In contrast, naively optimizing cross-entropy over the full  $\mathbb{Y}^V \times \mathbb{Y}^O$  space severely hurts unseen composition accuracy by treating most unseen compositions as negatives throughout training.

**Effects of penalty set in CPR.** In Table 5 (d), we study the effect of the penalty set  $\mathbb{Y}_{pen}$ . Compared to disabling  $L_{CPR}$ , penalizing *frequent* hard negatives ( $\mathbb{Y}_{hard} \cap \mathbb{Y}_{freq}$ ) yields the best trade-off, improving unseen composition accuracy and achieving the highest H.M. of 37.7%. In contrast, penalizing all hard negatives degrades object prediction and hurts overall composition performance, suggesting that restricting penalties to frequent confounders is critical.

**Table 5: Ablation study on the Sth-com [20] validation set.** We use C2C [20] with the CLIP [34] backbone as our baseline, using the unbiased open-world setting. We report performance on both seen and unseen compositions, along with their harmonic mean (H.M.). V@S and V@U denotes verb@seen-comp and verb@unseen-comp, while O@S and O@U denotes object@seen-comp and object@unseen-comp accuracies.

(a) Effects of RCORE components.								(b) Effects of TORC components.									
CPR	TORC	Verb		Object		Composition		$L_{cos}$	$L_{cent}$	Verb		Object		Composition (OW)			
		V@S	V@U	O@S	O@U	Seen	Unseen			H.M.	V@S	V@U	O@S	O@U	Seen	Unseen	H.M.
		65.26	54.02	67.21	56.81	47.31	30.14	36.83			65.26	54.02	67.21	56.81	47.31	30.14	36.83
✓		63.95	54.05	63.97	59.52	43.09	33.22	37.51	✓		64.15	55.96	67.71	55.97	47.13	31.11	37.48
	✓	64.93	57.49	66.20	57.23	46.28	33.92	39.15		✓	64.84	54.82	67.57	56.23	47.46	30.84	37.39
✓	✓	67.06	58.13	63.67	58.66	45.00	35.16	<b>39.48</b>	✓	✓	64.93	57.49	66.20	57.23	46.28	33.92	<b>39.15</b>
(c) Effects of label space in CPR.								(d) Effects of penalty set in CPR.									
Label Space	Verb		Object		Composition		Penalty Set	$\Upsilon_{pen}$	Choice	Verb		Object		Composition			
	V@S	V@U	O@S	O@U	Seen	Unseen				H.M.	V@S	V@U	O@S	O@U	Seen	Unseen	H.M.
Closed-world ( $\Upsilon_{seep}$ )	64.61	54.26	67.21	57.46	46.78	30.80	37.14			64.17	54.55	63.60	58.70	42.74	33.05	37.28	
Full Open-world ( $\Upsilon^s \times \Upsilon^o$ )	67.36	45.01	68.49	52.29	50.72	17.34	25.85			61.95	57.22	47.99	49.05	31.85	30.82	31.33	
Batch-adaptive ( $\Upsilon_{exp}$ )	64.17	54.55	63.60	58.70	42.74	33.05	<b>37.28</b>			65.36	55.86	63.20	57.62	43.60	33.16	<b>37.67</b>	

## 6 Conclusions

In this work, we revisit ZS-CAR and identify *object-driven shortcuts* as a key failure mode, driven by compositional sparsity and asymmetric verb-object learning difficulty. Using our diagnostic metrics, we show that existing models overfit to co-occurrence priors and consequently generalize poorly to unseen compositions. We propose RCORE with CPR (synthesized supervision with frequent hard-negative regularization) and TORC (temporal-order sensitivity), and demonstrate consistent gains on two benchmarks under open-world evaluation without test-tuned calibration.

## Acknowledgments

This work was supported by the NAVER Cloud Corporation and partly supported by the Institute of Information & Communications Technology Planning & Evaluation(IITP) grant funded by the Korea Government (MSIT) under grant RS-2024-00353131 and ITRC(Information Technology Research Center) grant funded by the Korea government(MSIT)(IITP-2025-RS-2023-00259004). Additionally, it was supported by the National Research Foundation of Korea(NRF) grant funded by the Korea government(MSIT)(RS-2025-02216217) and (RS-2025-22362968).

## References

1. Abbasi, R., Rohban, M.H., Baghshah, M.S.: Deciphering the role of representation disentanglement: Investigating compositional generalization in clip models. In: ECCV (2024) 4
2. Agrawal, A., Batra, D., Parikh, D., Kembhavi, A.: Don't just assume; look and answer: Overcoming priors for visual question answering. In: CVPR (2018) 4
3. Bae, K., Ahn, G., Kim, Y., Choi, J.: Devias: Learning disentangled video representations of action and scene for holistic video understanding. In: ECCV (2024) 1, 4

4. Bahng, H., Chun, S., Yun, S., Choo, J., Oh, S.J.: Learning de-biased representations with biased representations. In: ICML (2020) [4](#), [7](#)
5. Bai, S., Chen, K., Liu, X., Wang, J., Ge, W., Song, S., Dang, K., Wang, P., Wang, S., Tang, J., et al.: Qwen2.5-vl technical report. arXiv preprint arXiv:2502.13923 (2025) [4](#)
6. Chatterjee, D., Sener, F., Ma, S., Yao, A.: Opening the vocabulary of egocentric actions. In: NeurIPS (2023) [3](#), [4](#)
7. Choi, J., Gao, C., Messou, J.C., Huang, J.B.: Why can't i dance in the mall? learning to mitigate scene bias in action recognition. In: NeurIPS (2019) [4](#), [7](#)
8. Damen, D., Doughty, H., Farinella, G.M., Furnari, A., Ma, J., Kazakos, E., Moltisanti, D., Munro, J., Perrett, T., Price, W., Wray, M.: Rescaling egocentric vision: Collection, pipeline and challenges for epic-kitchens-100. IJCV **130**, 33–55 (2022) [1](#), [2](#), [3](#), [11](#), [19](#), [21](#)
9. Diba, A., Fayyaz, M., Sharma, V., Paluri, M., Gall, J., Stiefelhagen, R., Van Gool, L.: Large scale holistic video understanding. In: ECCV (2020) [1](#)
10. Ding, S., Li, M., Yang, T., Qian, R., Xu, H., Chen, Q., Wang, J., Xiong, H.: Motion-aware contrastive video representation learning via foreground-background merging. In: CVPR (2022) [4](#), [9](#), [25](#), [30](#)
11. Dosovitskiy, A., Beyer, L., Kolesnikov, A., Weissenborn, D., Zhai, X., Unterthiner, T., Dehghani, M., Minderer, M., Heigold, G., Gelly, S., Uszkoreit, J., Houlsby, N.: An image is worth 16x16 words: Transformers for image recognition at scale. In: ICLR (2021) [7](#), [22](#), [24](#)
12. Geirhos, R., Rubisch, P., Michaelis, C., Bethge, M., Wichmann, F.A., Brendel, W.: Imagenet-trained cnns are biased towards texture; increasing shape bias improves accuracy and robustness. In: ICLR (2018) [2](#), [4](#), [7](#)
13. Goyal, R., Kahou, S.E., Michalski, V., Materzynska, J., Westphal, S., Kim, H., Haanel, V., Fruend, I., Yianilos, P., Mueller-Freitag, M., et al.: The "something something" video database for learning and evaluating visual common sense. In: ICCV (2017) [1](#), [11](#), [21](#), [34](#)
14. Hu, E.J., Shen, Y., Wallis, P., Allen-Zhu, Z., Li, Y., Wang, S., Wang, L., Chen, W.: Lora: Low-rank adaptation of large language models. In: ICLR (2022) [8](#), [13](#), [14](#), [25](#), [29](#), [32](#)
15. Ilyas, A., Santurkar, S., Tsipras, D., Engstrom, L., Tran, B., Madry, A.: Adversarial examples are not bugs, they are features. In: NeurIPS (2019) [4](#)
16. Jiang, D., Jing, H., Ma, Y., Zheng, N.: Beyond image classification: A video benchmark and dual-branch hybrid discrimination framework for compositional zero-shot learning. In: CVPR (2025) [1](#), [4](#), [11](#), [31](#), [32](#)
17. Jung, H., Bak, J.H., Jeong, Y., Lee, G., Ahn, J., Kim, E.S.: Zero-shot compositional video learning with coding rate reduction. In: ICCV (2025) [1](#), [4](#), [8](#), [11](#), [12](#), [13](#), [31](#), [32](#)
18. Kim, H., Lee, J., Park, S., Sohn, K.: Hierarchical visual primitive experts for compositional zero-shot learning. In: ICCV (2023) [4](#), [31](#)
19. Li, K., Wang, Y., Li, Y., Wang, Y., He, Y., Wang, L., Qiao, Y.: Unmasked teacher: Towards training-efficient video foundation models. In: ICCV (2023) [4](#)
20. Li, R., Feng, Z., Xu, T., Li, L., Wu, X.J., Awais, M., Atito, S., Kittler, J.: C2c: Component-to-composition learning for zero-shot compositional action recognition. In: ECCV (2024) [1](#), [2](#), [3](#), [4](#), [5](#), [6](#), [7](#), [8](#), [10](#), [11](#), [12](#), [13](#), [14](#), [15](#), [19](#), [21](#), [22](#), [23](#), [25](#), [26](#), [27](#), [28](#), [29](#), [30](#), [31](#), [32](#), [33](#)
21. Li, Y., Li, Y., Vasconcelos, N.: Resound: Towards action recognition without representation bias. In: ECCV (2018) [2](#), [7](#)

22. Li, Y., Liu, Z., Chen, H., Yao, L.: Context-based and diversity-driven specificity in compositional zero-shot learning. In: CVPR (2024) [4](#), [31](#)
23. Liu, H., Li, C., Wu, Q., Lee, Y.J.: Visual instruction tuning. In: NeurIPS (2023) [4](#)
24. Loshchilov, I., Hutter, F.: Decoupled weight decay regularization. In: ICLR (2019) [26](#)
25. Luo, Z., Ghosh, S., Guillory, D., Kato, K., Darrell, T., Xu, H.: Disentangled action recognition with knowledge bases. In: North American Chapter of the Association for Computational Linguistics (2022) [4](#)
26. Ma, Y., Xu, G., Sun, X., Yan, M., Zhang, J., Ji, R.: X-clip: End-to-end multi-grained contrastive learning for video-text retrieval. In: ACM MM (2022) [4](#)
27. Mancini, M., Naeem, M.F., Xian, Y., Akata, Z.: Open world compositional zero-shot learning. In: CVPR (2021) [4](#), [31](#)
28. Materzynska, J., Xiao, T., Herzig, R., Xu, H., Wang, X., Darrell, T.: Something-else: Compositional action recognition with spatial-temporal interaction networks. In: CVPR (2020) [1](#), [2](#), [3](#), [11](#)
29. Misra, I., Gupta, A., Hebert, M.: From red wine to red tomato: Composition with context. In: CVPR (2017) [4](#)
30. Naeem, M.F., Xian, Y., Tombari, F., Akata, Z.: Learning graph embeddings for compositional zero-shot learning. In: CVPR (2021) [4](#)
31. Nam, J., Cha, H., Ahn, S., Lee, J., Shin, J.: Learning from failure: De-biasing classifier from biased classifier. In: NeurIPS (2020) [2](#), [4](#), [7](#)
32. Nayak, N.V., Yu, P., Bach, S.: Learning to compose soft prompts for compositional zero-shot learning. In: ICLR (2023) [4](#), [31](#)
33. Purushwalkam, S., Nickel, M., Gupta, A., Ranzato, M.: Task-driven modular networks for zero-shot compositional learning. In: ICCV (2019) [4](#), [31](#)
34. Radford, A., Kim, J.W., Hallacy, C., Ramesh, A., Goh, G., Agarwal, S., Sastry, G., Askell, A., Mishkin, P., Clark, J., et al.: Learning transferable visual models from natural language supervision. In: ICML (2021) [4](#), [6](#), [7](#), [8](#), [11](#), [12](#), [13](#), [15](#), [23](#), [24](#), [25](#), [26](#), [28](#), [30](#), [31](#)
35. Saini, N., Pham, K., Shrivastava, A.: Disentangling visual embeddings for attributes and objects. In: CVPR (2022) [4](#)
36. Scimeca, L., Oh, S.J., Chun, S., Poli, M., Yun, S.: Which shortcut cues will DNNs choose? a study from the parameter-space perspective. In: ICLR (2022) [2](#), [4](#), [7](#)
37. Sevilla-Lara, L., Zha, S., Yan, Z., Goswami, V., Feiszli, M., Torresani, L.: Only time can tell: Discovering temporal data for temporal modeling. In: WACV (2021) [11](#), [33](#), [34](#)
38. Singh, K.K., Mahajan, D., Grauman, K., Lee, Y.J., Feiszli, M., Ghadiyaram, D.: Don't judge an object by its context: learning to overcome contextual bias. In: CVPR (2020) [2](#), [4](#)
39. Sun, P., Wu, B., Li, X., Li, W., Duan, L., Gan, C.: Counterfactual debiasing inference for compositional action recognition. In: ACM MM (2021) [3](#)
40. Wang, J., Gao, Y., Li, K., Lin, Y., Ma, A.J., Cheng, H., Peng, P., Huang, F., Ji, R., Sun, X.: Removing the background by adding the background: Towards background robust self-supervised video representation learning. In: CVPR (2021) [4](#)
41. Wang, Y., Li, K., Li, X., Yu, J., He, Y., Wang, C., Chen, G., Pei, B., Zheng, R., Xu, J., Wang, Z., et al.: Internvideo2: Scaling video foundation models for multimodal video understanding. ECCV (2024) [2](#), [4](#), [5](#), [6](#), [7](#), [8](#), [11](#), [12](#), [13](#), [24](#), [25](#), [26](#), [32](#), [33](#)
42. Wu, P., Lai, Q., Fang, H., Xie, G.S., Yin, Y., Lu, X., Wang, W.: A conditional probability framework for compositional zero-shot learning. In: ICCV (2025) [4](#), [31](#)

43. Yang, T., Zhu, Y., Xie, Y., Zhang, A., Chen, C., Li, M.: Aim: Adapting image models for efficient video understanding. In: ICLR (2023) [5](#), [8](#), [12](#), [13](#), [14](#), [25](#), [29](#), [32](#)
44. Ye, G., Li, L., Li, K., Xiao, J., Chen, L.: Zero-shot compositional action recognition with neural logic constraints. In: ACM MM (2025) [1](#), [4](#), [31](#), [32](#)
45. Yun, S., Han, D., Oh, S.J., Chun, S., Choe, J., Yoo, Y.: Cutmix: Regularization strategy to train strong classifiers with localizable features. In: ICCV (2019) [25](#)
46. Yun, S., Kim, J., Han, D., Song, H., Ha, J.W., Shin, J.: Time is matter: Temporal self-supervision for video transformers. In: ICML (2022) [11](#), [12](#), [33](#)
47. Zhang, H., Cisse, M., Dauphin, Y.N., Lopez-Paz, D.: mixup: Beyond empirical risk minimization. In: ICLR (2018) [25](#), [30](#)
48. Zhang, T., Liang, K., Du, R., Chen, W., Ma, Z.: Disentangling before composing: Learning invariant disentangled features for compositional zero-shot learning. TPAMI **47**(2), 1132–1147 (2024) [4](#)
49. Zhao, L., Gundavarapu, N.B., Yuan, L., Zhou, H., Yan, S., Sun, J.J., Friedman, L., Qian, R., Weyand, T., Zhao, Y., Hornung, R., Schroff, F., Yang, M.H., Ross, D.A., Wang, H., Adam, H., Sirotenko, M., Liu, T., Gong, B.: Videoprism: A commercial-grade video foundation model. In: ICML (2024) [4](#)
50. Zhou, K., Yang, J., Loy, C.C., Liu, Z.: Learning to prompt for vision-language models. IJCV **130**(9), 2337–2348 (2022) [25](#)

## Appendix

In this appendix, we provide comprehensive evaluation-protocol/ dataset/implementation details and additional results to complement the main paper. We organize the appendix as follows:

1. Overview of our evaluation setting (Section A).
2. Details on EK100-com dataset (Section B).
3. Complete implementation details (Section C).
4. Additional evidence of object-driven shortcuts (Section D).
5. Additional results (Section E).

### A Overview of our evaluation setting

In Figure 7 and Figure 8, we briefly describe our evaluation setting. In Zero-Shot Compositional Action Recognition (ZS-CAR), the compositional label space spans the Cartesian product of the verb and object primitives ( $|\mathbb{Y}^V| \times |\mathbb{Y}^O|$ ). At test time, samples are categorized into *seen* and *unseen* compositions depending on whether they were observed during training, as shown in Figure 7 (a). Under the *closed-world* evaluation setting, the evaluation is restricted to compositions present within the dataset (i.e., the union of the training and test sets). Consequently, the model computes compositional logits exclusively for these predefined closed-world pairs, as shown in Figure 7 (b).

However, this *closed-world* setting suffers from the impractical assumption of requiring prior knowledge of the test set’s ground-truth labels. Therefore, we adopt the *open-world* evaluation setting as our primary protocol. By evaluating across the entire compositional space and computing logits for all possible combinations, as shown in Figure 7 (b), the open-world setting enables the evaluation of various possible-but-unseen compositions encountered in real-world applications, where the test distribution is unknown.

As shown in Figure 8, we measure verb, object, and composition accuracies across seen and unseen splits to evaluate not only the model’s compositional recognition capability, but also how primitive recognition degrades on unseen compositions. Specifically, based on the model’s composition predictions, we verify whether the composition, verb, or object is predicted correctly, yielding three sets of metrics: (1) seen/unseen composition accuracy, (2) verb@seen/unseen-comp, and (3) object@seen/unseen-comp.

### B Details on EK100-com dataset

In this section, we provide details about our curated ZS-CAR benchmark, EPIC-KITCHENS-100-composition (EK100-com). We construct EK100-com by repurposing EPIC-KITCHENS-100 (EK100) [8] following the same protocol of constructing Sth-com [20]. In particular, we use the original training (67,217 samples) and validation (9,668 samples) split of EK100 [8] and split them as follows:

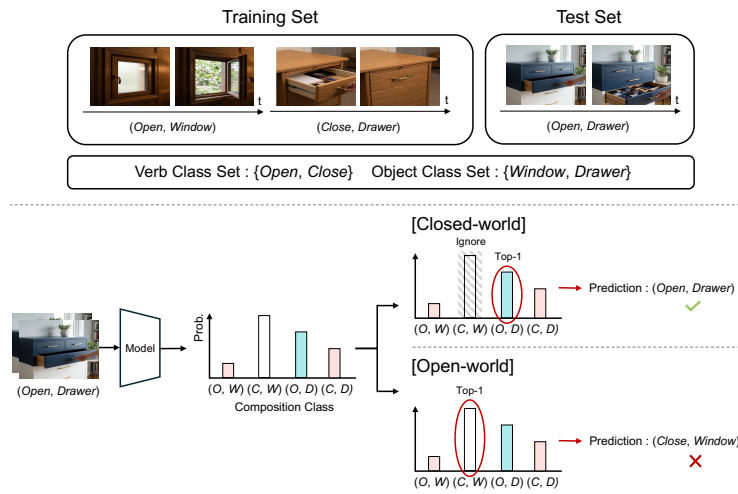
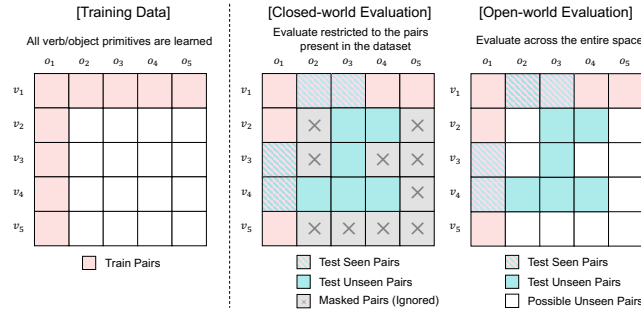


**Fig. 7: Closed-world and open-world evaluation protocols in ZS-CAR.** (a) (Left) Primitives are learned from a subset of training compositions (*Train Pairs*). (Middle) Closed-world evaluation restricts inference to dataset-present pairs (*Train Pairs* and *Test Seen/Unseen Pairs*), explicitly ignoring others as *Masked Pairs*. (Right) Open-world evaluation spans the entire compositional space, requiring the model to navigate all *Possible Unseen Pairs* without artificial masking. (b) In the closed-world setting, the *Possible Unseen Pair*—not appearing in the dataset—(*Close, Window*) becomes a *Masked Pair*, and its logit is ignored. Consequently, the next valid class (*Open, Window*) is selected as the top-1 prediction. This closed-world setting constrains the evaluation of numerous possible-but-unseen compositions. However, in the open-world setting, the model treats all pairs as valid, thus predicting (*Close, Window*) as the top-1 prediction.

(1) we filter the data to include only compositions with more than five samples each. (2) we ensure that all compositions present in the validation set also exist in the training set. After initial filtering, the training set comprises 62,790 samples with 1,331 unique compositions and the validation set contains 8,657 samples,

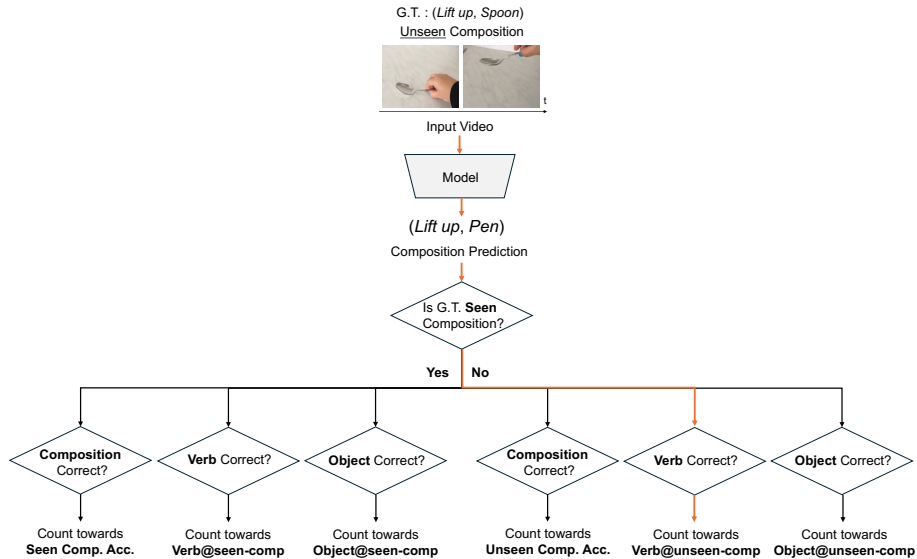


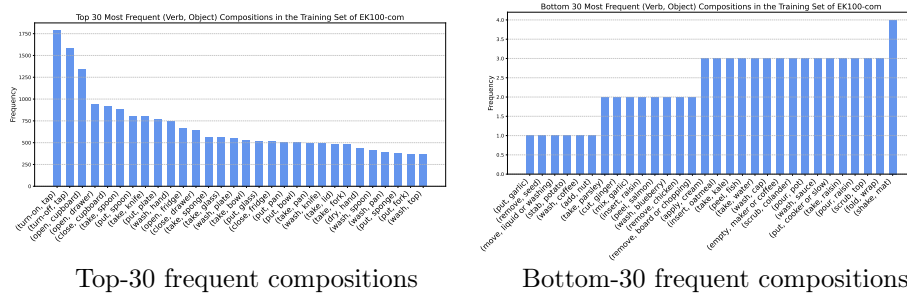
**Fig. 8: Evaluation metrics used in this work.** We evaluate accuracies for verbs, objects, and compositions on seen and unseen composition splits separately. Based on the model’s composition predictions, we count the correct matches at each level to report (1) seen/unseen composition accuracy, (2) verb@seen/unseen-comp, and (3) object@seen/unseen-comp. For instance, predicting an unseen composition (*Lift up, Spoon*) as (*Lift up, Pen*) updates only the correct count for verb@unseen-comp (orange arrow).

which consist of 833 seen compositions and 3 unseen compositions. (3) we randomly select half of the compositions from both the training and validation sets and swap these subsets. (4) Finally, we split the validation and test set with a ratio of 3 : 4. We provide the statistics of EK100-com in Table 6 and Figure 9, and some seen/unseen composition examples of EK100-com in Figure 10.

Beyond expanding the pool of publicly available ZS-CAR benchmarks, our repurposed EK100-com exhibits two key properties that make it a compelling ZS-CAR benchmark. First, unlike Something-Something V2 [13], where videos may involve multiple objects associated with a verb, videos in EK100 [8] depict actions consisting of a single verb and a single object. Therefore, the training data of EK100-com provides explicit object supervision for the models. Second, since EK100 [8] has long-tailed distribution, the label coverage ratio—defined as the number of unique verb-object pairs present in the dataset relative to all possible combinations—of EK100-com is 7.5%, which is much lower than that of Sth-com [20] (12.8%). This makes EK100-com a challenging benchmark, suitable for evaluating whether a model can overcome the risk of shortcut learning induced by data sparsity.

**Table 6: Details of the our introduced EK100-com benchmark.** The label coverage ratio of EK100-com is  $7.5\% = 1320/(81 \times 216)$ .

EK100-com #	Verb #	Object	# Compositions	# Samples
Train	81	216	1133	54691
Val	57	175	462 Seen & 187 Unseen	3085 Seen & 4007 Unseen
Test	61	177	522 Seen & 187 Unseen	4197 Seen & 5258 Unseen
Total	81	216	1320	71238

**Fig. 9: Top/Bottom-30 frequent compositions in the EK100-com training set.**

## C Complete Implementation Details

### C.1 Implementation details on our diagnosis

In this section, we provide comprehensive details of experimental setup and implementation details of our diagnosis for ZS-CAR in Section 3. All notations used in this appendix are consistent with those defined in the main paper. As mentioned in Section 3, we adopt the state-of-the-art model, C2C [20], as the existing ZS-CAR baseline for diagnosis.

**Details about our diagnosis in Figure 2 (a).** In Figure 2 (a) in the main paper, we empirically demonstrate the asymmetric learning difficulty between verbs and objects. We train a randomly initialized ViT [11] with joint Spatio-Temporal (ST) attention on our selected subset of the Sth-com [20] dataset. We aim to select a dense subset that eliminates sparsity by ensuring samples exist for every pair, maximizing the number of samples while maintaining a sufficient number of distinct labels. As a result, the selected subset is composed of 10 verb classes: ‘Moving sth and sth away from each other’, ‘Moving sth and sth closer to each other’, ‘Moving sth away from sth’, ‘Moving sth closer to sth’, ‘Moving sth down’, ‘Moving sth up’, ‘Pushing sth from left to right’, ‘Pushing sth from right to left’, ‘Pushing sth so that it falls off the table’, and ‘Pushing sth so that it slightly moves’; and 10 object classes: ‘Ball’, ‘Battery’, ‘Book’, ‘Bottle’, ‘Coin’, ‘Glass’, ‘Knife’, ‘Paper’, ‘Remote’, and ‘Spoon’. We construct the training set consisting of 2,555 samples from the original Sth-Com [20] training and validation samples, while the validation set comprises 260 samples from the original Sth-Com [20] test set. For training, we employ a multi-task learning

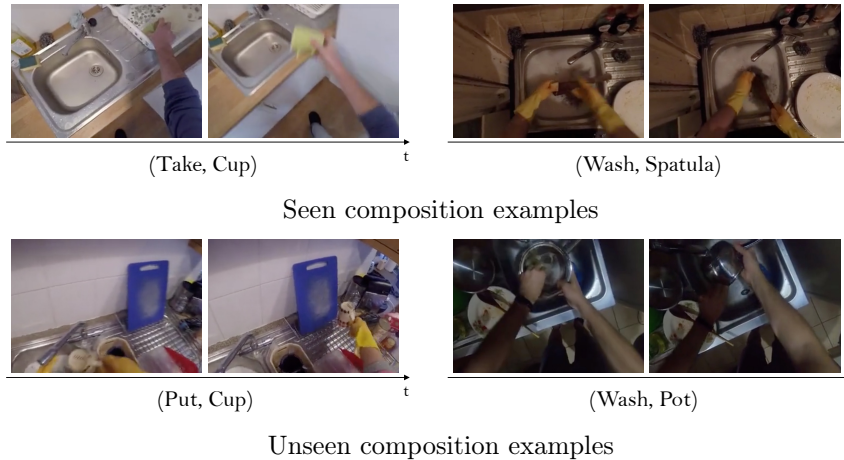


**Fig. 10: Example of seen/unseen composition samples in the EK100-com dataset.**

approach using separate linear classifiers for verbs and objects, taking the ViT’s CLS token as input.

**Details about our diagnosis in Figure 2 (b).** To precisely control the sample counts for each verb-object pair, we select a  $4 \times 4$  toy set from the Sth-Com [20] dataset. This set contains four verb labels (‘Moving sth down’, ‘Moving sth up’, ‘Pushing sth from left to right’, and ‘Pushing sth from right to left’) and four object labels (Book, Remote, Glass, Bottle). As shown in Figure 2 and Figure 11, the training set consists of the four diagonal pairs with 40 samples per pair. The test set comprises two distinct splits: seen compositions (25 samples per pair) and unseen compositions (30 samples per pair). We use 8 frames for input videos. In Figure 11, we demonstrate that the object-driven verb shortcut learning observed with CLIP [34] in the main paper emerges identically even in a randomly initialized model. This indicates that this phenomenon is not a side effect of pre-trained knowledge, but rather a structural issue inherent to ZS-CAR.

**Details about our diagnosis in Figure 3.** In Figure 3, we present the learning curves of the baseline model [20] trained on the Sth-com [20]. We further present diagnostic results for both the baseline and RCORE on EK100-com in Figure 12. We define two misclassification ratios, False Seen Prediction (FSP) and False Co-occurrence Prediction (FCP). FSP measures the proportion of unseen composition validation samples incorrectly classified as seen compositions:

$$\text{False Seen Prediction} = \frac{1}{|\mathbb{D}_{\text{val}}^{\text{unseen}}|} \sum_{i=1}^{|\mathbb{D}_{\text{val}}^{\text{unseen}}|} \mathbb{I}(\hat{\mathbf{y}}_i^C \in \mathbb{Y}_{\text{seen}}), \quad (9)$$

where  $\mathbb{I}(\cdot)$  is the indicator function. FCP further quantifies the fraction of these false-seen predictions that correspond to frequently co-occurring verb-object

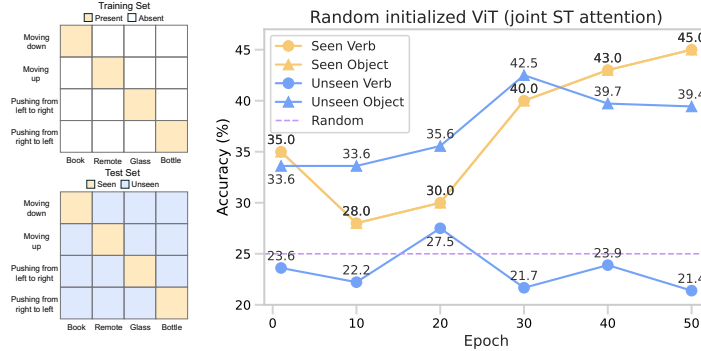


**Fig. 11: Object-driven shortcuts with the random initialized model.** Even with a randomly initialized model, a ViT-B [11] with joint ST attention, *object-driven shortcuts emerge*: the model achieves high object accuracy, but verb accuracy on bias-conflicting unseen compositions drops below chance, indicating shortcut-driven verb failures.

pairs  $\mathbb{Y}_{\text{freq}}$  in the training data:

$$\text{False Co-oc. Prediction} = \frac{1}{|\mathbb{D}_{\text{val}}^{\text{unseen}}|} \sum_{i=1}^{|\mathbb{D}_{\text{val}}^{\text{unseen}}|} \mathbb{I}(\hat{\mathbf{y}}_i^C \in \mathbb{Y}_{\text{freq}}). \quad (10)$$

We further break down these misclassification ratios into the three cases: (i) Verb-collapse, where the predicted object is correct but the verb is incorrect; (ii) Object-collapse, where the predicted verb is correct but the object is incorrect; and (iii) Dual-collapse, where both verb and object are incorrect. We define them in FSP as follows:

$$\text{Verb-collapse} = \frac{\sum_{i=1}^{|\mathbb{D}_{\text{val}}^{\text{unseen}}|} \mathbb{I}(\hat{\mathbf{y}}_i^C \in \mathbb{Y}_{\text{freq}}) \cdot \mathbb{I}(\hat{\mathbf{y}}_i^V \neq \mathbf{y}_i^V \wedge \hat{\mathbf{y}}_i^O = \mathbf{y}_i^O)}{\sum_{i=1}^{|\mathbb{D}_{\text{val}}^{\text{unseen}}|} \mathbb{I}(\hat{\mathbf{y}}_i^C \in \mathbb{Y}_{\text{freq}})} \quad (11)$$

$$\text{Object-collapse} = \frac{\sum_{i=1}^{|\mathbb{D}_{\text{val}}^{\text{unseen}}|} \mathbb{I}(\hat{\mathbf{y}}_i^C \in \mathbb{Y}_{\text{freq}}) \cdot \mathbb{I}(\hat{\mathbf{y}}_i^V = \mathbf{y}_i^V \wedge \hat{\mathbf{y}}_i^O \neq \mathbf{y}_i^O)}{\sum_{i=1}^{|\mathbb{D}_{\text{val}}^{\text{unseen}}|} \mathbb{I}(\hat{\mathbf{y}}_i^C \in \mathbb{Y}_{\text{freq}})} \quad (12)$$

$$\text{Dual-collapse} = \frac{\sum_{i=1}^{|\mathbb{D}_{\text{val}}^{\text{unseen}}|} \mathbb{I}(\hat{\mathbf{y}}_i^C \in \mathbb{Y}_{\text{freq}}) \cdot \mathbb{I}(\hat{\mathbf{y}}_i^V \neq \mathbf{y}_i^V \wedge \hat{\mathbf{y}}_i^O \neq \mathbf{y}_i^O)}{\sum_{i=1}^{|\mathbb{D}_{\text{val}}^{\text{unseen}}|} \mathbb{I}(\hat{\mathbf{y}}_i^C \in \mathbb{Y}_{\text{freq}})}, \quad (13)$$

where  $\mathbf{y}_i^C = (\mathbf{y}_i^V, \mathbf{y}_i^O)$ . We apply the identical formulation for FCP as well.

## C.2 Implementation details on RCORE

**Experimental Setup.** We implement our method using PyTorch and conduct all experiments on 8 NVIDIA Tesla V100 GPUs. For video preprocessing, we uniformly sample frames from each video to generate clips of size  $3 \times 16 \times 224 \times 224$  (channels  $\times$  frames  $\times$  height  $\times$  width) for the CLIP [34] backbone and  $3 \times 8 \times 224 \times 224$  for the InternVideo2 [41] backbone.

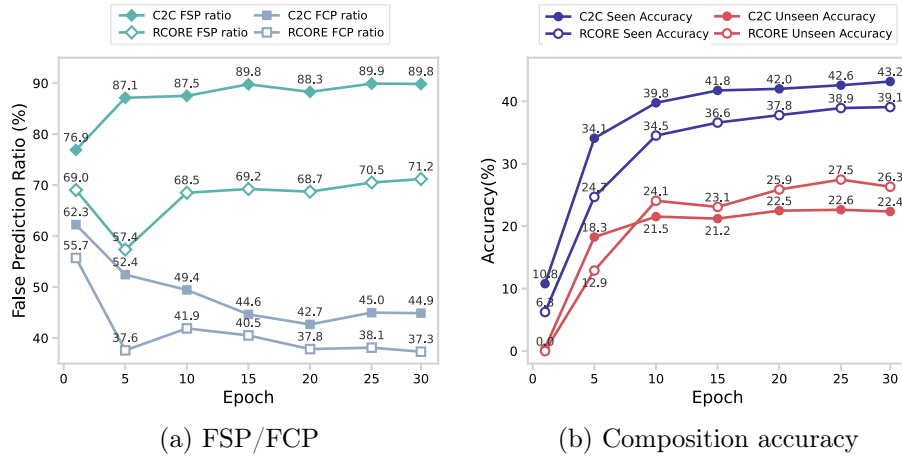


**Fig. 12: Learning curve of the baseline and RCORE on EK100-com.** RCORE (a) suppresses the increase of FCP during training, (b) effectively narrowing the performance gap between seen and unseen composition validation accuracies, compared to the baseline (C2C [20]).

**Model Architecture.** We utilize CLIP-B/16 [34] as our visual/text backbone. Following prior work [20], we adopt AIM [43], a parameter-efficient spatio-temporal adapter for CLIP [34], as the video encoder. We also employ InternVideo2-CLIP-B/14 [41] as our modern video-pretrained VLM backbone and utilize LoRA [14] for parameter-efficient fine-tuning. We use CoOp-style [50] learnable text prompts for all models. We also construct the verb encoder with two temporal convolution layers with ReLU activations, while the object encoder employs temporal average pooling followed by a two-layer MLP with ReLU activations.

To extract  $T$  frame-level features with the InternVideo2 [41] backbone, we modify its attention pooling mechanism. Originally, the model concatenates a CLS token with video tokens in  $\mathbb{R}^{NT \times D}$ , where  $N$  is the number of spatial patches and  $D$  is the feature dimension, and applies attention pooling to produce a single video-level representation in  $\mathbb{R}^{1 \times D}$ . In our approach, we adapt this to operate at the frame level. Specifically, for each frame, we concatenate the CLS token with the corresponding spatial tokens in  $\mathbb{R}^{N \times D}$ . This creates  $T$  separate feature sets, each in  $\mathbb{R}^{(N+1) \times D}$ . Finally, we apply attention pooling independently to each of these sets, resulting in the frame-level video features in  $\mathbb{R}^{T \times D}$ .

**Training Strategy.** We train all models, including the baselines and RCORE, following the hyperparameters detailed in Table 7, using a total batch size of 128. For CPR, we employ the unsupervised foreground estimation algorithm FAME [10] to identify high-motion regions. FAME [10] isolates the moving foreground from background regions based on frame differences and color statistics. To generate the mixed samples, we first sample the mixing coefficient from a Beta(2.0, 2.0) distribution, following prior work [45, 47]. We then scale it by 0.5 to obtain the final blending coefficient  $\lambda$ . We apply this CPR’s augmentation to the samples within a batch with a probability of  $p_{\text{aug}}$ . For the frequent

**Table 7: Hyperparameters used for training RCORE on each dataset.** We denote InternVideo2 [41] as ‘IV2’.

Config	Sth-com [20]		EK100-com	
	CLIP [34]	IV2 [41]	CLIP [34]	IV2 [41]
Optimizer	AdamW [24]			
Base learning rate (visual)	5e-4	5e-5	1e-4	5e-5
Base learning rate (text)	1e-4	5e-5	1e-5	5e-5
Weight decay (visual)	1e-4			
Weight decay (text)	1e-5			
Optimizer momentum	$\beta_1, \beta_2 = 0.9, 0.999$			
Per GPU batch size	16			
Warmup epochs	3			
$\alpha, \beta, \gamma, \delta$	0.2, 1.0, 1.0, 0.1			
$p_{CPR}$	0.95	0.8	0.95	0.8
(start, end) epoch for scaling $\gamma$	(5, 10)			
(start, end) epoch for scaling $\delta$	(15, 15)	(30, 35)	(35, 40)	(30, 35)
Scale factor for $\lambda$ in CPR	0.5			
Softmax temperature	0.07			
Training epochs	40	50	40	40

verb-object pairs to apply the  $L_{CPR}$  loss term, we select pairs that possess a strong co-occurrence prior from both verb and object perspectives as the frequent pairs  $\mathbb{Y}_{\text{freq}}$ , which is defined as  $\mathbb{Y}_{\text{freq}} = \mathbb{Y}_{\text{freq}}^{O|V} \cap \mathbb{Y}_{\text{freq}}^{V|O}$ .  $\mathbb{Y}_{\text{freq}}^{O|V}$  is the set of pairs where the conditional probability of an object given a verb in the training data is greater than  $\mu + \sigma$ . Here,  $\mu$  and  $\sigma$  represent the mean and standard deviation of the conditional probabilities calculated on the training set. The  $\mathbb{Y}_{\text{freq}}^{V|O}$  is defined similarly for the conditional probability of a verb given an object. ( $\mu_{O|V} + \sigma_{O|V}, \mu_{V|O} + \sigma_{V|O}$ ) are calculated as (0.13, 0.19) for the Sth-com [20] dataset and (0.23, 0.40) for EK100-com.

**Loss configuration.** For the total loss, we set the weights for the verb and object components to  $\alpha = 0.2$  and for the composition loss to  $\beta = 1.0$ , following prior work [20]. As demonstrated in Table 11 (d), we empirically find it beneficial to linearly warm up the weights for the TORC loss:  $\gamma$  is increased from 0.0 to 1.0 over 5 epoch to 10 epoch. We use  $\delta$ , the loss scale of  $L_{CPR}$ , differently depending on the dataset and backbone, as detailed in Table 7.

**Inference.** During inference, we adopt a single-view, single-crop protocol. To select the best model during training and for bias calibration, we use the harmonic mean of the accuracies for seen and unseen compositions as the model selection criterion.

## D Additional evidence of object-driven shortcuts

In this section, we provide further evidence demonstrating that existing ZS-CAR learning approaches are susceptible to object-driven shortcut learning.

**Failure case analysis of the existing ZS-CAR model.** In Table 8 and Table 9, we investigate top-10 failure cases of the model trained with the state-of-the-art method [20]. The top-10 failure cases shown in the Table 8 constitute 9.5% of the misclassifications on unseen compositions for Sth-com [20], compared

**Table 8: Top-10 failure cases of the existing ZS-CAR model on unseen compositions of the Sth-com test set.** We employ C2C [20] trained on Sth-com [20] as baseline for analysis. We use ‘sth’ instead of ‘something’ to shorten. We report the results with unbiased open-world inference scores. ‘Prediction Rate’ denotes the proportion of mispredictions classified as the specific composition. ‘Verb/Object-side’ indicates the most frequently co-occurring counterpart for each mispredicted component in the training set, along with its co-occurrence ratio. The top-10 cases listed below account for 9.5% of the total mispredictions on unseen compositions.

Rank	Ground Truth (Verb, Object)	Error Count / Rate (%)	Top-2 Misprediction (seen/unseen)	Prediction Count / Rate (%)	Most Frequent Co-occurring Component During Training
					Verb-side / Object-side
1	(‘Pretending to be tearing [sth] that is not tearable’, ‘Paper’)	192 / 99.0%	(‘Tearing [sth] just a little bit’, ‘Paper’) (seen) (‘Folding [sth]’, ‘Paper’) (seen)	116 / 60.4% 47 / 24.5%	w/ ‘Paper’ (71.6%) w/ ‘Tearing [sth] just a little bit’ (26.7%) w/ ‘Paper’ (41.9%) w/ ‘Tearing [sth] just a little bit’ (26.7%)
2	(‘Unfolding [sth]’, ‘Paper’)	140 / 44.7%	(‘Folding [sth]’, ‘Paper’) (seen) (‘Tearing [sth] into two pieces’, ‘Paper’) (unseen)	80 / 27.1% 12 / 8.6%	w/ ‘Paper’ (41.9%) w/ ‘Tearing [sth] just a little bit’ (26.7%) w/ ‘Envelope’ (17.4%) w/ ‘Tearing [sth] just a little bit’ (26.7%)
3	(‘Opening [sth]’, ‘Box’)	106 / 82.8%	(‘Showing that [sth] is inside [sth]’, ‘Box’) (seen) (‘Showing that [sth] is empty’, ‘Box’) (seen)	27 / 25.5% 23 / 21.7%	w/ ‘Box’ (22.7%) w/ ‘Showing that [sth] is empty’ (10.1%) w/ ‘Cup’ (30.8%) w/ ‘Showing that [sth] is empty’ (10.1%)
4	(‘Spacing [sth]’, ‘Plastic bag’)	94 / 40.9%	(‘Spacing [sth]’, ‘Bag’) (seen) (‘Folding [sth]’, ‘Plastic bag’) (unseen)	77 / 81.9% 13 / 13.8%	w/ ‘Sponge’ (11.8%) w/ ‘Stuffing [sth] into [sth]’ (14.4%) w/ ‘Paper’ (43.9%) w/ ‘[sth] falling like a feather or paper’ (57.4%)
5	(‘Putting [sth] into [sth]’, ‘Box’)	88 / 68.3%	(‘Stuffing [sth] into [sth]’, ‘Box’) (seen) (‘Putting [sth] into [sth]’, ‘Plastic box’) (seen)	10 / 11.4% 8 / 9.1%	w/ ‘Box’ (19.2%) w/ ‘Showing that [sth] is empty’ (10.1%) w/ ‘Bowl’ (12.4%) w/ ‘Closing [sth]’ (25.9%)
6	(‘Lifting up one end of [sth], then letting it drop down’, ‘Card’)	79 / 54.1%	(‘Lifting [sth] up completely without letting it drop down’, ‘Card’) (unseen) (‘Lifting up one end of [sth], then letting it drop down’, ‘Pencil’) (unseen)	30 / 25.3% 19 / 24.1%	w/ ‘Crayon’ (26.8%) w/ ‘Uncovering [sth]’ (19.8%) w/ ‘Crayon’ (26.8%) w/ ‘Uncovering [sth]’ (13.7%)
7	(‘Putting [sth] on a surface’, ‘Bottle’)	77 / 68.1%	(‘Putting [sth] upright on the table’, ‘Bottle’) (seen) (‘Hitting [sth] with [sth]’, ‘Bottle’) (seen)	33 / 42.9% 15 / 19.5%	w/ ‘Bottle’ (42.1%) w/ ‘Turning [sth] upside down’ (5.3%) w/ ‘Bottle’ (14.8%) w/ ‘Turning [sth] upside down’ (5.3%)
8	(‘Showing that [sth] is empty’, ‘Bottle’)	70 / 85.4%	(‘Turning [sth] upside down’, ‘Bottle’) (seen) (‘Pretending to turn [sth] upside down’, ‘Bottle’) (seen)	17 / 18.6% 8 / 11.4%	w/ ‘Bottle’ (21.7%) w/ ‘Turning [sth] upside down’ (5.3%) w/ ‘Bottle’ (30.6%) w/ ‘Turning [sth] upside down’ (5.3%)
9	(‘Throwing [sth]’, ‘Book’)	69 / 84.2%	(‘[sth] falling like a rock’, ‘Book’) (seen) (‘Throwing [sth]’, ‘Hat’) (seen)	16 / 23.2% 9 / 13.0%	w/ ‘Bottle’ (13.0%) w/ ‘Pushing [sth] from left to right’ (4.9%) w/ ‘Tissue’ (7.7%) w/ ‘Throwing [sth]’ (25.0%)
10	(‘Closing [sth]’, ‘Drawer’)	60 / 69.0%	(‘Opening [sth]’, ‘Drawer’) (seen) (‘Stuffing [sth] into [sth]’, ‘Drawer’) (seen)	21 / 35.7% 6 / 10.0%	w/ ‘Door’ (18.9%) w/ ‘Opening [sth]’ (36.8%) w/ ‘Box’ (19.2%) w/ ‘Opening [sth]’ (36.8%)

**Table 9: Top-10 failure cases of the existing ZS-CAR model on unseen compositions of the EK100-com test set.** We employ C2C [20] trained on EK100-com as baseline for analysis. We report the results with unbiased open-world inference scores. ‘Prediction Rate’ denotes the proportion of mispredictions classified as the specific composition. ‘Verb/Object-side’ indicates the most frequently co-occurring counterpart for each mispredicted component in the training set, along with its co-occurrence ratio. The top-10 cases listed below account for  $\sim 39\%$  of the total mispredictions on unseen compositions.

Rank	Ground Truth (Verb, Object)	Error Count / Rate (%)	Top-2 Misprediction (seen/unseen)	Prediction Count / Rate (%)	Most Frequent Co-occurring Component
					Verb-side / Object-side
1	(‘put’, ‘knife’)	340 / 80.8%	(‘take’, ‘knife’) (seen) (‘put’, ‘fork’) (seen)	81 / 23.8% 41 / 12.1%	w/ ‘spoon’ (6.8%) w/ ‘take’ (56.2%) w/ ‘spoon’ (8.6%) w/ ‘take’ (40.3%)
2	(‘put’, ‘lid’)	303 / 76.7%	(‘take’, ‘lid’) (seen) (‘remove’, ‘lid’) (seen)	44 / 14.5% 22 / 7.3%	w/ ‘spoon’ (6.8%) w/ ‘take’ (45.4%) w/ ‘lid’ (16.1%) w/ ‘take’ (45.4%)
3	(‘take’, ‘plate’)	259 / 46.7%	(‘put’, ‘plate’) (seen) (‘take’, ‘bowl’) (seen)	70 / 27.0% 32 / 12.4%	w/ ‘spoon’ (8.6%) w/ ‘put’ (52.1%) w/ ‘spoon’ (6.8%) w/ ‘take’ (32.6%)
4	(‘wash’, ‘sink’)	143 / 100%	(‘wash’, ‘top’) (seen) (‘wash’, ‘cloth’) (seen)	68 / 47.6% 14 / 9.8%	w/ ‘hand’ (12.7%) w/ ‘wash’ (89.2%) w/ ‘hand’ (12.7%) w/ ‘take’ (35.2%)
5	(‘put’, ‘spatula’)	131 / 69.0%	(‘take’, ‘spatula’) (seen) (‘put’, ‘spoon’) (seen)	42 / 32.1% 18 / 13.7%	w/ ‘spoon’ (6.8%) w/ ‘take’ (58.2%) w/ ‘spoon’ (6.8%) w/ ‘take’ (36.9%)
6	(‘put’, ‘cup’)	115 / 56.1%	(‘take’, ‘cup’) (seen) (‘put’, ‘glass’) (seen)	25 / 21.7% 11 / 9.6%	w/ ‘spoon’ (6.8%) w/ ‘take’ (48.8%) w/ ‘spoon’ (8.6%) w/ ‘take’ (36.4%)
7	(‘shake’, ‘hand’)	94 / 97.9%	(‘turn-off’, ‘tap’) (seen) (‘wash’, ‘hand’) (seen)	38 / 40.4% 18 / 19.1%	w/ ‘tap’ (93.6%) w/ ‘turn-on’ (49.5%) w/ ‘hand’ (12.7%) w/ ‘wash’ (59.8%)
8	(‘put’, ‘board or chopping’)	89 / 56.0%	(‘take’, ‘board or chopping’) (seen) (‘put’, ‘knife’) (unseen)	11 / 12.4% 9 / 10.1%	w/ ‘spoon’ (6.8%) w/ ‘take’ (45.1%) w/ ‘spoon’ (8.6%) w/ ‘take’ (56.2%)
9	(‘wash’, ‘hob’)	83 / 70.9%	(‘wash’, ‘top’) (seen) (‘wash’, ‘oven’) (seen)	38 / 45.8% 7 / 10.3%	w/ ‘hand’ (12.7%) w/ ‘wash’ (89.2%) w/ ‘hand’ (12.7%) w/ ‘open’ (35.9%)
10	(‘take’, ‘salt’)	74 / 70.5%	(‘put’, ‘salt’) (seen) (‘pour’, ‘salt’) (seen)	9 / 12.2% 7 / 9.5%	w/ ‘spoon’ (8.6%) w/ ‘put’ (38.0%) w/ ‘water’ (25.2%) w/ ‘put’ (37.9%)

to 49% for EK100-com as shown in Table 9. For the analysis of Sth-com [20], we exclude ambiguous cases arising from annotation issues to obtain meaningful results. A prime example is the top-1 failure case, (‘Covering [something] with [something]’, ‘Paper’), where 66% of the errors are misclassified as ‘Pencil’. Upon visual inspection, we confirm that nearly all these videos actually depict

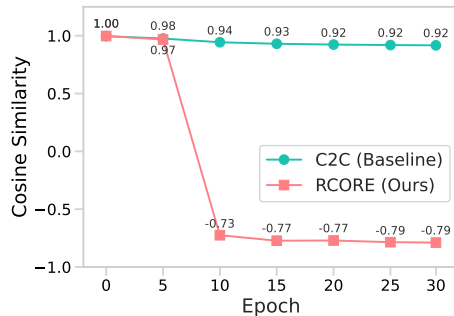


**Fig. 13: Similarity analysis between original and reversed verb features.** We plot the cosine similarity between the original and reversed verb features for the baseline (C2C [20]) and RCORE with the CLIP [34] backbone on the Sth-com [20] dataset. The baseline maintains a *high similarity* (+0.92) during entire training, revealing limited temporal sensitivity. In contrast, the similarity becomes *strongly negative* for RCORE as training progresses, indicating improved temporal discriminative capability.

the action of covering a pencil with paper. In Table 8 and Table 9, we observe a common tendency across both datasets: the model frequently misclassifies verbs as their temporally reversed or opposing counterparts. Specifically, we demonstrate that these mispredictions stem from the model’s reliance on co-occurrence statistics. For instance, the model misclassifies unseen ‘(Closing, Drawer)’ samples as ‘(Opening, Drawer)’, which accounts for 36% of the errors. Notably, ‘Opening’ is the verb most frequently paired with ‘Drawer’ in the training set. These findings suggest that the model has failed to learn robust verb representations that generalize to unseen compositions, largely due to object-driven shortcut learning.

**Similarity analysis of verb features.** In Figure 13, we track the cosine similarity between the original verb features  $\mathbf{f}^V$  and the reversed verb features  $\mathbf{f}_{\text{rev}}^V$  for the baseline [20] over the course of training. The baseline [20] maintains a high cosine similarity (+0.92), revealing its reliance on object-driven shortcuts rather than temporally grounded verb representations. Additionally, we plot the similarity of RCORE in Figure 13. RCORE drives this similarity to a strongly negative value (−0.79), indicating that the model successfully distinguishes opposite temporal semantics, *e.g.* ‘opening’ *vs.* ‘closing’.

**Table 10: Macro Compositional Gap results.** We show Macro Compositional Gap ( $\Delta_{CG}^{\text{macro}}$ ) results of C2C [20] and RCORE on the Sth-com [20] and EK100-com datasets. The **best** numbers are highlighted.

Backbone	Method	Sth-com		EK100-com	
		Seen	Unseen	Seen	Unseen
CLIP	AIM [43]	+1.18	-0.47	+0.95	-1.10
	C2C [20]	+0.78	+0.16	+1.56	-0.38
	RCORE	+0.53	+0.64	-0.03	+0.11
InternVideo2	LoRA [14]	0.00	-0.16	+0.60	-0.53
	C2C [20]	+0.59	+0.14	+0.83	-0.38
	RCORE	-0.33	+0.76	+0.02	+0.85

## E Additional Results

### E.1 Macro Compositional Gap

In this section, we define Macro Compositional Gap ( $\Delta_{CG}^{\text{macro}}$ ).  $\Delta_{CG}^{\text{macro}}$  is the macro version of Compositional Gap ( $\Delta_{CG}$ ), which averages  $\Delta_{CG}$  per composition class, ensuring robustness to class imbalance. Let  $\mathbb{Y}_{\text{test}}^C \subseteq \mathbb{Y}^V \times \mathbb{Y}^O$  denote the set of *unique* composition labels that appear in the test split. For each  $\mathbf{y}^C = (\mathbf{y}^V, \mathbf{y}^O) \in \mathbb{Y}_{\text{test}}^C$ , let  $\text{Acc}_{\mathbf{y}^C}^C$  be the top-1 composition accuracy restricted to samples of  $\mathbf{y}^C$ , and let  $\text{Acc}_{\mathbf{y}^C}^V$  and  $\text{Acc}_{\mathbf{y}^C}^O$  be the corresponding verb/object accuracies on the same samples of  $\mathbf{y}^C$ , computed from the joint top-1 composition predictions. Then we define

$$\Delta_{CG}^{\text{macro}} = \frac{1}{|\mathbb{Y}_{\text{test}}^C|} \sum_{\mathbf{y}^C \in \mathbb{Y}_{\text{test}}^C} \left[ \text{Acc}_{\mathbf{y}^C}^C - \left( \text{Acc}_{\mathbf{y}^C}^V \times \text{Acc}_{\mathbf{y}^C}^O \right) \right]. \quad (14)$$

In Table 10, we report  $\Delta_{CG}^{\text{macro}}$  performances of baselines and RCORE on the Sth-com [20] and EK100-com datasets. RCORE consistently achieves the highest  $\Delta_{CG}^{\text{macro}}$  on unseen compositions across different backbones and datasets, demonstrating its robust compositional reasoning capabilities.

### E.2 Additional ablation results

In Table 11, we provide the comprehensive ablation study results to examine each design choice of RCORE, using the Sth-com [20] dataset.

**Effects of TORC with different temporal aggregation methods.** In Table 11 (a), we demonstrate that the weak temporal order modeling caused by object-driven shortcut learning cannot be resolved merely by employing more sophisticated temporal aggregation methods. We compare the baseline’s temporal average pooling with attention pooling (Attn. pool). In attention pooling, a linear layer computes frame-wise attention weights from the input verb feature sequences, aggregating them via a weighted sum to obtain the final verb feature for classification. While attention pooling yields a slight improvement in verb accuracy, it fails to reduce the compositional gap ( $\Delta_{CG}$ ) on unseen compositions. In contrast, our TORC achieves significant improvements in harmonic

**Table 11: Additional ablation study of RCore on Sth-com.** We provide the additional ablation study results on Sth-com [20]. In every experiment, we use C2C [20] with CLIP-B/16 [34] as our baseline. We report performance on both seen and unseen compositions, along with their harmonic mean (H.M.). The **best** numbers are highlighted.

(a) Effects of TORC with different temporal aggregation.									(b) Effects of input samples in CPR.									
Method	TORC	Verb		Object		Composition			Inputs	Verb		Object		Composition				
		V@S	V@U	O@S	O@U	Seen ( $\Delta_{CG}$ )	Unseen ( $\Delta_{CG}$ )	H.M.		V@S	V@U	O@S	O@U	Seen	Unseen	H.M.		
Average	×	63.60	54.36	67.72	56.10	46.31	(+3.24)	30.08	(-0.42)	36.47	Original	62.54	52.97	56.90	57.05	37.43	31.41	34.16
Attn. pool	×	64.28	54.76	67.50	55.73	47.11	(+3.72)	30.09	(-0.43)	36.72	Mixup [47]	62.37	52.56	63.50	59.20	41.62	31.45	35.83
Average	✓	65.65	56.80	68.59	55.19	48.65	(+3.62)	31.35	(-0.00)	<b>38.13</b>	CPR w/o F.E. [10]	63.23	54.29	65.15	56.49	43.57	30.86	36.13
Attn. pool	✓	65.51	56.50	67.80	55.00	48.07	(+3.65)	30.78	(-0.30)	37.53	CPR w/ F.E. [10]	64.17	54.55	63.60	58.70	42.74	33.05	<b>37.28</b>

(c) Effects of hyperparameters of CPR.								(d) Effects of hyperparameters of TORC.									
$p_{CPR}$	Verb		Object		Composition			$\gamma$	scaling		Verb		Object		Composition		
	V@S	V@U	O@S	O@U	Seen	Unseen	H.M.		start epoch	end epoch	V@S	V@U	O@S	O@U	Seen	Unseen	H.M.
0.8	64.66	52.89	65.06	58.77	45.20	31.14	36.88	0.5	1	1	65.59	55.63	68.49	54.80	48.33	30.19	37.17
0.9	64.70	55.50	64.73	57.69	44.75	32.60	<b>37.72</b>	1.0	1	1	64.88	55.81	67.21	55.12	47.06	30.69	37.15
0.95	63.95	54.05	63.97	59.52	43.09	33.22	37.51	1.0	5	5	64.93	56.03	67.67	55.81	47.20	31.38	37.70
1.0	64.95	55.50	61.49	57.20	41.82	32.84	36.79	1.0	5	10	65.65	56.80	68.59	55.19	48.65	31.35	<b>38.13</b>

(e) Effects of hyperparameters of $L_{CPR}$ .											
$m$	$\delta$	scaling		Verb		Object		Composition			
		start epoch	end epoch	V@S	V@U	O@S	O@U	Seen	Unseen	H.M.	
0.5	0.1	15	15	67.06	58.13	63.67	58.66	45.00	35.16	<b>39.48</b>	
0.5	0.1	15	20	66.16	58.78	63.75	57.96	44.65	34.89	39.17	
0.5	0.5	15	15	66.16	57.03	62.75	57.56	43.55	33.77	38.04	
0.5	0.5	15	20	67.04	56.77	61.74	57.56	43.37	34.30	38.31	
1.0	0.1	15	15	66.31	58.56	63.77	57.99	44.47	34.64	38.94	
1.0	0.1	15	20	66.88	58.24	63.88	57.01	44.90	34.21	38.83	

mean (H.M.) with both aggregation methods. Notably, the combination of temporal average pooling and TORC enables the model to overcome the negative compositional gap.

**Effects of input samples in CPR.** In Table 11 (b), we validate the effects of input sample types in CPR. We argue that conventional image-based augmentations are insufficient for representing newly created unseen composition labels. For example, Mixup [47] blends verbs and objects concurrently, failing to preserve the temporal difference information that is essential for verb recognition. As a result, these methods yield a lower verb@unseen-comp than the baseline (52.6% vs. 53.0%). In contrast, our CPR adopts a static frame mixing strategy, aiming to generate novel compositions by mixing only object information while preserving the verbs, shows modest performance gains over the baseline for both verb and object accuracy on unseen compositions, resulting in the best H.M. Furthermore, we observe that mixing a static frame into the estimated foreground region shows additional performance boost (+0.2 points in the H.M.) over applying it to the entire background, as it creates more realistic samples. We denote the latter as ‘CPR w/o F.E.’, indicating ‘without foreground estimation’.

**Effects of hyperparameters of RCore.** In Table 11 (c), we show the effect of  $p_{CPR}$ , the per-batch probability for CPR application, revealing a trade-off between seen and unseen composition accuracies. Decreasing  $p_{CPR}$  slightly from 1.0 (e.g. 0.95 or 0.9) yields optimal unseen accuracy improvements with minimal drops in seen performance, whereas lowering it further (e.g.  $p_{CPR} = 0.8$ )

**Table 12: Ablation study on EK100-com.** We provide the results of the ablation study on EK100-com presented in the main paper. In every experiment, we use C2C [20] with CLIP-B/16 [34] as our baseline. We report performance on both seen and unseen compositions, along with their harmonic mean (H.M.).

(a) Effects of CPR and TORC.								(b) Effects of each TORC loss term.									
CPR	TORC	Verb		Object		Composition		$L_{cos}$	$L_{ent}$	Verb		Object		Composition			
		V@S	V@U	O@S	O@U	Seen	Unseen			H.M.	V@S	V@U	O@S	O@U	Seen	Unseen	H.M.
		66.19	49.71	56.61	47.48	42.72	22.38	29.38			66.19	49.71	56.61	47.48	42.72	22.38	29.38
✓		66.06	51.28	54.23	50.56	38.93	27.10	31.96	✓		65.43	52.11	56.54	47.44	42.67	24.24	<b>30.92</b>
	✓	65.90	52.31	57.28	46.74	43.48	23.67	30.65		✓	66.00	51.06	56.64	47.37	42.82	22.53	29.53
✓	✓	67.52	54.08	54.00	49.04	40.13	27.40	<b>32.56</b>	✓	✓	65.90	52.31	57.28	46.74	43.48	23.67	30.65

(c) Effects of $L_{CPR}$ in CPR.							
$L_{CPR}$	Verb		Object		Composition		H.M.
	V@S	V@U	O@S	O@U	Seen	Unseen	
	66.35	50.79	54.72	50.16	39.25	26.60	31.71
✓	66.06	51.28	54.23	50.56	38.93	27.10	<b>31.96</b>

degrades the gains on unseen pairs. Consequently, we tune  $p_{CPR}$  for each dataset and backbone based on the best validation H.M. of seen and unseen accuracies, as shown in Table 7. In Table 11 (d), we observe that introducing the explicit temporal order modeling task via TORC starting from 5 epoch, after initial training, is effective. In particular, the strategy of linearly increasing the loss weight from epoch 5 to 10 is the most effective. Finally, in Table 11 (e), we analyze the impact of the loss weights of  $L_{CPR}$  in CPR. Increasing the margin  $m$  or loss weight  $\delta$  degrades performance, suggesting that excessive training penalties are detrimental. We find  $m = 0.5$  and  $\delta = 0.1$  to be optimal. Contrary to the results in Table 11 (d), maintaining a constant low loss weight ( $\delta = 0.1$ ) for  $L_{CPR}$  yields better performance than applying progressive weight scaling.

### E.3 Ablation studies on EK100-com

In Table 12, we provide the ablation study results conducted on the EK100-com dataset, complementing the results discussed with the Sth-com [20] dataset in the main paper. In Table 12 (a), we demonstrate that while CPR and TORC are individually effective, integrating both components yields the best performance on EK100-com, outperforming the baseline in H.M. by 3.2 points. In Table 12 (b), using only  $L_{cos}$  in TORC yields the highest H.M. on EK100-com. In Table 12 (c), suppressing co-occurrence priors with  $L_{cos}$  improves H.M. by 0.3 points, consistent with the results on Sth-com [20].

### E.4 Results with validation-set-tuned bias calibration

In this section, we provide the open-world biased results with validation-set-tuned calibration. *Bias calibration* is a standard technique in compositional zero-shot learning [18, 22, 27, 32, 33, 42] and ZS-CAR [16, 17, 20, 44]. It compensates for the inherent issue where logits for unseen compositions—not optimized during training—are naturally lower than those for seen compositions. Specifically, it

**Table 13: Sth-com results with bias calibration.** We show the top-1 verb, object, and composition classification accuracies (%) on the Sth-com [20] test set. We tune the bias term for unseen composition predictions on the validation set and apply the selected bias (‘Best Bias’) to the test set. We report performance on both seen and unseen compositions, along with their harmonic mean (H.M.). The **best** numbers are highlighted.

Backbone	Method	Best Bias	Verb			Object			Composition		
			@Seen Comp	@Unseen Comp	H.M.	@Seen Comp	@Unseen Comp	H.M.	Seen ( $\Delta_{CG}$ )	Unseen ( $\Delta_{CG}$ )	H.M.
CLIP	AIM [43]	+0.01	50.32	43.19	46.48	64.02	54.78	59.04	33.40 (+1.19)	24.60 (+0.94)	28.33
	C2C [20]	+0.07	60.97	56.62	58.71	65.05	56.98	60.75	42.06 (+2.40)	33.98 (+1.72)	37.59
	RCORE	0.00	65.73	59.00	<b>62.18</b>	64.79	56.34	60.27	<b>44.99 (+2.40)</b>	<b>33.90 (+0.66)</b>	<b>38.67</b>
InternVideo2	LoRA [14]	+0.02	42.02	40.74	41.37	64.04	59.75	61.82	26.00 (−0.91)	25.09 (+0.75)	25.54
	C2C [20]	+0.03	68.54	65.27	66.87	68.58	64.58	<b>66.52</b>	48.42 (+1.41)	42.66 (+0.51)	45.36
	RCORE	0.00	71.65	66.65	<b>69.06</b>	67.96	64.56	66.22	<b>50.20 (+1.51)</b>	<b>43.98 (+0.95)</b>	<b>46.88</b>

adds a scalar bias term exclusively to the unseen composition logits. Previous ZS-CAR works [16, 17, 20, 44] often tuned this bias using test-set ground truth under a closed-world setting to report the ‘best’ seen and unseen accuracies. We argue that this approach is highly unrealistic.

Instead, we adopt an open-world *validation-set-tuned* bias calibration. We tune the bias on the validation set using open-world logits and then apply it to the test set. This approach remains applicable to real-world scenarios while effectively improving unseen composition performance as a post-processing step.

In Table 13, we present the calibrated results of the baselines and RCORE on the Sth-com [20] dataset. Notably, the calibrated performance of RCORE is *identical* to its original unbiased performance. This indicates that our training label space expansion strategy via our proposed CPR is effective. Unlike baseline methods that overfit solely to seen compositions, it successfully provides meaningful supervision for unseen compositions during training. Furthermore, the *unbiased* performance of RCORE consistently outperforms the best calibrated performance of all baselines. This demonstrates that RCORE is highly suitable for real-world applications, delivering strong ZS-CAR performance without the need for any post-processing.

## E.5 Results with large video-pretrained VLM backbone

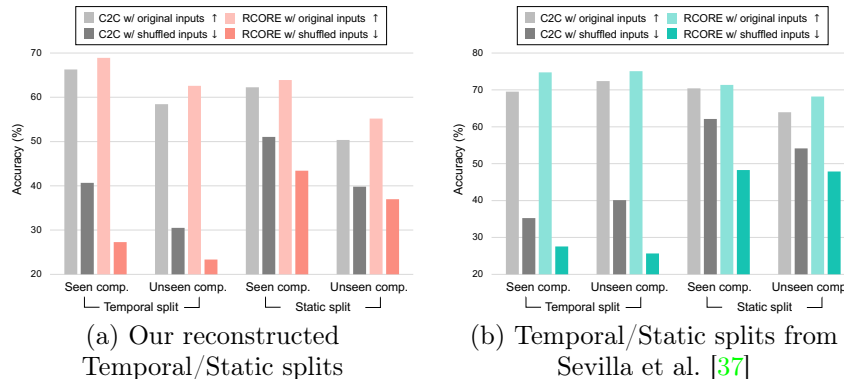
We compare RCORE and the baseline (C2C [20]) on Sth-com [20] and EK100-com using the InternVideo2-1B [41] backbone, whose 1B-parameter vision encoder is approximately  $11\times$  larger than the 87M-parameter vision encoders used in the main paper. In Table 14, RCORE yields consistent improvements over the baseline on Sth-com [20] and EK100-com, boosting unseen composition accuracy (+3.4p., +2.1p.), unseen  $\Delta_{CG}$  (+0.8p., +1.1p.), and H.M. (+1.5p., +0.4p.), respectively. These results demonstrate that its powerful representation learning capability is not constrained by the backbone’s parameter size.

**Table 14: Sth-com results with InternVideo2-1B.** We show the top-1 verb, object, and composition classification accuracies (%) on the Sth-com [20] and EK100-com datasets with the InternVideo2-1B [41] backbone. We report performance on both seen and unseen compositions, along with their harmonic mean (H.M.). The **best** numbers are highlighted.

Sth-com results										
Method	Verb			Object			Composition			
	@Seen Comp	@Unseen Comp	H.M.	@Seen Comp	@Unseen Comp	H.M.	Seen ( $\Delta_{CG}$ )	Unseen ( $\Delta_{CG}$ )	H.M.	
C2C [20]	67.50	58.21	62.51	70.58	61.62	65.80	50.23 (+2.59)	34.96 (-0.91)	41.23	
RCORE	67.49	60.47	63.79	68.83	63.63	66.13	48.27 (+1.82)	38.35 (-0.13)	<b>42.74</b>	

EK100-com results										
Method	Verb			Object			Composition			
	@Seen Comp	@Unseen Comp	H.M.	@Seen Comp	@Unseen Comp	H.M.	Seen ( $\Delta_{CG}$ )	Unseen ( $\Delta_{CG}$ )	H.M.	
C2C [20]	66.95	52.22	58.67	60.57	50.81	55.26	45.91 (+5.36)	26.66 (+0.13)	33.73	
RCORE	66.36	52.88	58.86	56.83	52.10	54.36	41.86 (+4.16)	28.79 (+1.24)	<b>34.12</b>	



**Fig. 14: Performances on Temporal/Static split of Sth-com.** We evaluate the models on Sth-com [20] using both (a) our reconstructed splits and (b) the splits from Sevilla et al [37]. We utilize both original and temporally shuffled inputs to assess the model’s temporal modeling capability and its reliance on static cues. A larger performance gap between original and shuffled inputs indicates that the model predicts verbs more based on temporal dynamics rather than on static cues.

## E.6 Temporal/Static split of Sth-com

We present extended results corresponding to the experiment shown in Figure 5 (c) of the main paper, including all versions of the Temporal/Static split. Inspired by prior work [37, 46], we rigorously evaluate the temporal modeling capabilities by partitioning the Sth-com [20] dataset into Temporal and Static splits, as shown in Figure 14. We evaluate both the baseline (C2C [20]) and RCORE on the two types of splits, (i) our reconstructed splits and (ii) the splits proposed by Sevilla et al. [37]. In all cases, RCORE exhibits lower performance on shuffled

inputs but outperforms the baseline on original inputs. This indicates that RCORE predicts verbs without relying on static cues, leading to robust improvements in verb performance regardless of the split.

In this paragraph, we describe the differences between two Temporal/Static splits. Sevilla et al. [37] originally defined these splits based on cognitive science experiments on Something-Something V2 [13] verb classes: a Temporal split (18 verbs) where temporal information matters, and a Static split (18 verbs) where such information is redundant. However, noting that this Static split includes verbs requiring complex temporal reasoning such as ‘Folding’, we reconfigure the splits based on verb semantics. Specifically, we categorized verbs based on this criterion: those requiring temporal information for discrimination are assigned to the Temporal split (62 verbs), while verbs distinguishable by momentary keyframes are assigned to the Static split (80 verbs). The indices of the verbs in the Temporal split are as follows: 0, 1, 5, 6, 14, 25, 26, 29, 30, 32, 33, 34, 35, 38, 39, 40, 41, 42, 43, 44, 45, 46, 58, 59, 60, 61, 65, 66, 67, 68, 72, 73, 74, 75, 76, 78, 79, 85, 86, 90, 91, 92, 98, 100, 103, 109, 122, 123, 131, 134, 136, 137, 139, 140, 145, 146, 147, 148, 149, 150, 153, 154. The indices of the verbs in the Static split are as follows: 2, 3, 8, 9, 10, 11, 12, 13, 15, 16, 17, 18, 19, 20, 21, 22, 23, 24, 27, 28, 31, 36, 37, 47, 48, 49, 50, 51, 52, 53, 54, 55, 77, 80, 81, 87, 88, 93, 94, 95, 96, 97, 99, 101, 102, 104, 105, 106, 110, 111, 112, 113, 114, 115, 116, 117, 118, 119, 120, 121, 126, 127, 128, 129, 130, 132, 133, 135, 138, 141, 142, 143, 151, 152, 155, 156, 157, 158, 159, 160. To balance the sample sizes between the Temporal and Static splits, we excluded a few verbs with the fewest samples from the Temporal split.